Quaternary Research (2017), **87**, 227–245.

doi:10.1017/qua.2016.14

Late Holocene hydroclimatic change at Cienega Amarilla, west-central New Mexico, USA

Jill Onken[a]*, Susan J. Smith[b], Manuel R. Palacios-Fest[c], Karen R. Adams[d]

[a]Department of Geosciences, University of Arizona, 1040 E. 4th St., Tucson, Arizona 85721, USA
[b]Consulting Archaeopalynologist, 8875 Carefree Ave., Flagstaff, Arizona 86004, USA
[c]Terra Nostra Earth Sciences Research, P.O. Box 37195, Tucson, Arizona 85740, USA
[d]Archaeobotanical Consultant, 2837 E. Beverly Dr., Tucson, Arizona 85716, USA

(Received December 8, 2015; Accepted December 6, 2016)

Abstract

A late Holocene carbonate spring mound and associated wetland deposits at Cienega Amarilla, New Mexico, contain a 4000-yr record of geomorphic, paleoenvironmental, and hydroclimatic change on the southern Colorado Plateau. Forty-four ^{14}C dates support a century-scale chronostratigraphic framework. Pollen, plant macrofossil, mollusk, ostracode, and soil analyses indicate rapid spring mound growth and wetland expansion beginning ~2300 cal yr BP, followed by a pronounced decline in groundwater discharge (GWD) between ~1500 and 1000 cal yr BP. The isotopic composition of Cienega Amarilla springwater suggests GWD is driven primarily by winter precipitation. Historical climate data indicate that El Niño and warm Pacific Decadal Oscillation (PDO) conditions foster wetter-than-average winters in the Cienega Amarilla area, whereas dry winters are associated with La Niña conditions regardless of PDO phase. The ~2300–1500 cal yr BP Cienega Amarilla pluvial appears to represent an interval of peak, late Holocene cool-season precipitation that implies unusually strong or persistent El Niño–like and warm PDO–like conditions in the Pacific. Other southwestern paleoenvironmental records corroborate atypically wet conditions during this interval, and pluvial conditions related to increased winter precipitation likely fostered significant prehistoric cultural changes throughout the region, including increased sedentism, population, and dependence on agriculture.

Keywords: Late Holocene; Alluvial stratigraphy; Paleowetlands; Paleoclimatology; Colorado Plateau; Carbon-14; El Niño; Pacific Decadal Oscillation; Geoarchaeology

INTRODUCTION

Cienega Amarilla is a spring-fed wetland with a large, late Holocene carbonate spring mound located on the southern Colorado Plateau in west-central New Mexico near the Arizona state line (Fig. 1). Spring mound features of Holocene age are relatively rare in the southwestern United States. Past shifts in spring discharge often reflect paleohydrologic and paleoclimatic variability (Kreamer and Springer, 2008; Pigati et al., 2014), and the Cienega Amarilla stratigraphic record—which includes alluvium and groundwater discharge (GWD) deposits—is therefore an important archive of local and regional paleoenvironmental and hydroclimatic change. GWD deposits can provide information about the timing and magnitude of past episodes of heightened water tables related to moister and/or cooler conditions (Pigati et al., 2014). A distinct period of rapid spring mound growth and wetland expansion at Cienega Amarilla signifies a late Holocene interval of elevated water tables and increased spring discharge.

The Cienega Amarilla record is significant because of its potential to help clarify hydroclimatic relationships on the southern Colorado Plateau, including the underlying causes of past pluvials and droughts, as well as possible effects of future climate change on the region's limited water resources. Objectives of this study included identifying and characterizing stratigraphic units and depositional facies in the Cienega Amarilla vicinity, establishing a high-resolution (centennial-scale) chronostratigraphic framework using extensive radiocarbon dating, and reconstructing local paleoenvironmental conditions by utilizing pollen, plant macrofossil, mollusk, ostracode, and soil analyses. Because winter rainfall and snow are more effective than summer rains in recharging water tables in the southwestern United States (Eastoe et al., 2004; Haynes, 2008; Wagner et al., 2010), another objective of this study was to evaluate the hypothesis that the Holocene

*Corresponding author at: Department of Geosciences, University of Arizona, 1040 E. 4th St., Tucson, AZ 85721, United States. E-mail address: jonken@email.arizona.edu (J. Onken).

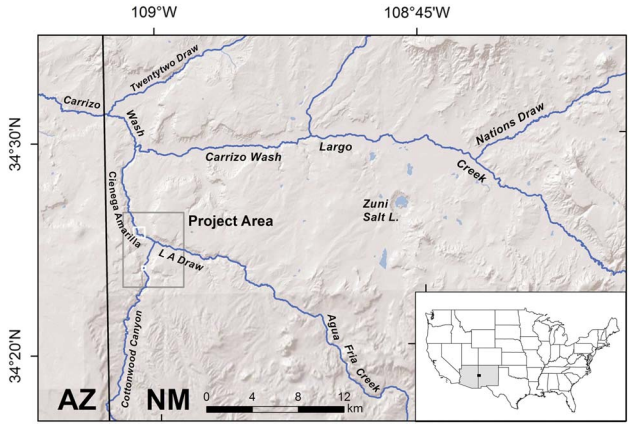

Figure 1. (color online) Location map of study area. Cienega Amarilla and Cottonwood Canyon subareas illustrated in Figure 2 are outlined in white. Inset map shows location of project area within the conterminous United States as small black rectangle, with Arizona and New Mexico shaded gray.

hydroclimatic history of Cienega Amarilla spring discharge was driven largely by changes in winter precipitation.

Geologic and hydrologic context

Cienega Amarilla is located between the Springerville and Red Hill–Quemado volcanic fields and coincides with the Jemez lineament, a northeast-trending zone of crustal weakness and normal faulting (Mayo, 1958; Magnani et al., 2004). Bedrock in the Cienega Amarilla vicinity consists primarily of Triassic Chinle Formation capped by Upper Cretaceous Dakota Sandstone. These sedimentary rock units dip slightly (1°) to the north, forming the northern limb of a gentle anticline (O'Brien, 1956). The hydrostratigraphic and geologic conditions that give rise to the Cienega Amarilla springs have not been studied. However, the springs may be fed by one or more aquifers—including the Shinarump Conglomerate, Kaibab Limestone, and Coconino Sandstone—that underlie the floodplain and are confined between a Chinle Formation shale member and Supai Formation red beds (O'Brien, 1956; Akers, 1964).

Although geologic maps (O'Brien, 1956; New Mexico Bureau of Geology and Mineral Resources, 2003) and satellite imagery show no definitive evidence of faulting at Cienega Amarilla, northeast-trending normal faults have been documented 13 km to the southeast (Chamberlain et al., 1994), and it is possible that the Cienega Amarilla springs are related to undocumented, buried faults. Cienega Amarilla is ~20–40 km east of extensive, middle to late Pleistocene (36–354 ka) travertine deposits related to a large natural CO_2 gas field trapped under a broad anticline (Embid, 2009). Cienega Amarilla lies ~6 km outside the mapped extent of the CO_2 field (Moore et al., 2005), and it is unclear what, if any, relationship exists between the recent Cienega Amarilla carbonate deposits and these older travertine deposits.

Cienega Amarilla (~1930 m above mean sea level) is situated immediately below the confluence of Cottonwood Canyon and LA Draw (Fig. 1). This study focused on a 1.4 km reach of Cienega Amarilla and a 600-m reach of Cottonwood Canyon that is ~3 km south and ~40 m higher in the watershed. The ~1500 km^2 Cienega Amarilla watershed extends to elevations of 2860 m and constitutes roughly one-quarter of the catchment of Carrizo Wash, a headwater tributary of the Little Colorado River. The groundwater catchment feeding the Cienega Amarilla springs is undefined and does not necessarily coincide with the surface drainage basin extent. In general, however, groundwater in the Coconino Sandstone and Kaibab Limestone aquifers is recharged by rain and snowmelt in the White Mountains and Mogollon Rim areas to the south (including areas outside Cienega Amarilla's surface drainage catchment) and moves northward, largely controlled by regional dip (Akers, 1964).

The ~3-m-high carbonate spring mound at Cienega Amarilla presently covers 9 hectares (0.09 km^2) and is inactive (Fig. 2a). Historical-period arroyo cutting during the late nineteenth or early twentieth century removed the mound's western margin, and today the Cienega Amarilla floodplain is entrenched by an arroyo as much as 11 m deep and 80 m wide. In contrast, arroyos in Cottonwood Canyon are substantially narrower and shallower (Fig. 2b). According to local rancher Clifford A. Thorn (personal communication, 2011), arroyo cutting began in the 1890s when heavy rains triggered gullying of wagon trail ruts created by early homesteaders running sheep in the area. This is consistent with widespread arroyo formation in the southwest United States at this time (Waters and Haynes, 2001), including entrenchment of the Zuni River (~50 km to the north) between 1879 and 1899 (Hall et al., 2009). Historical incision of the Cienega Amarilla floodplain probably caused spring flow at mound orifice(s) to cease. A series of springs, however, presently issue from the arroyo bottom into confined pools and marshes, resulting in perennial flow along a 2- to 3-km-long reach of the drainage.

Lower elevation streams in the Carrizo Wash watershed are alluvial systems characterized by ephemeral flow (Basabilvazo, 1997), and perennial flow along the Cienega Amarilla reach is a unique exception. Cienega Amarilla presently supports a narrow corridor of riparian and aquatic plants within its entrenched channel, including willow (*Salix* sp.), cottonwood (*Populus fremontii*), tamarisk (invasive *Tamarix* sp.), bulrush (*Scirpus* sp.), cattail (*Typha* sp.), sedges (Cyperaceae), and a variety of herbaceous plants and grasses. These wetland phreatophytes differ dramatically from the surrounding xeric vegetation dominated by four-wing saltbush (*Atriplex canescens*), juniper (*Juniperus monosperma*), and a variety of grasses. The carbonate spring mound supports an unusual vegetation community that includes New Mexico privet (*Forestiera neomexicana*), skunkbush (*Rhus trilobata*), and wolfberry (*Lycium* sp.).

Climate

Modern climate in the Cienega Amarilla area is semiarid and mesic, with moderately seasonal precipitation and strongly seasonal temperatures. Mean annual precipitation is weakly bimodal, with more than half resulting from warm-season

https://doi.org/10.1017/qua.2016.14 Published online by Cambridge University Press

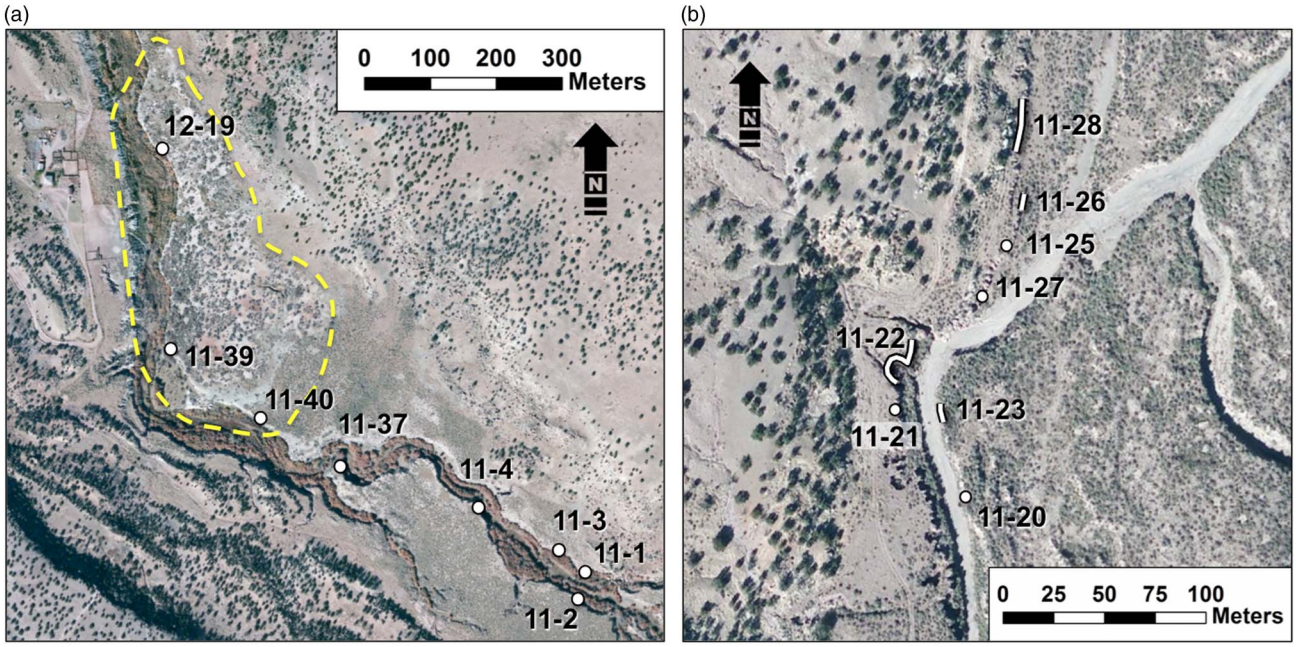

Figure 2. (color online) Satellite imagery showing Cienega Amarilla (a) and Cottonwood Canyon (b) profile locations. Dashed line outlines estimated original extent of spring mound.

(July–September) storms, including intense, localized North American monsoon (NAM) thunderstorms and less frequent, more widespread tropical cyclones (Smith, 1986; Dean, 1988; Adams and Comrie, 1997; Western Regional Climate Center, 2016). Because Cienega Amarilla lies south of most winter westerly storm tracks, winters are generally relatively dry. Large cyclonic storms or a southerly shifted jet stream, however, can result in widespread winter precipitation over the southwestern United States (for a detailed discussion, see Sheppard et al., 2002). Winter precipitation in the Southwest is largely linked to the El Niño–Southern Oscillation (ENSO), which is driven by sea-surface temperature (SST) and surface air pressure fluctuations between the eastern and western tropical Pacific Ocean (Andrade and Sellers, 1988; Wang et al., 2016). During El Niño events, the Pacific storm track shifts southward, and the southwestern United States generally experiences wetter, cooler winters than average, whereas La Niña winters tend to be drier and warmer (Kiladis and Diaz, 1989; Trenberth et al., 1998). Southwest winters are also influenced by northern Pacific SST temporal variation known as the Pacific Decadal Oscillation (PDO). The PDO alternates between positive (warmer) and negative (colder) phases every 20–30 yr, in contrast with the 2–10 yr ENSO cycle. Colder PDO phases are linked to winter drought in the Southwest, but warm PDO phases often enhance El Niño winter precipitation in this region (Sheppard et al., 2002).

METHODS

Fieldwork involved documenting 16 stratigraphic profiles. Arroyos provided extensive natural exposures, and profile locations were selected based on accessibility and the presence of fresh, vertical exposures and datable material. Three profiles are along the western margin of the Cienega Amarilla spring mound where modern arroyo cutting and widening has removed part of the mound (Fig. 2a). Five other profiles are upstream and southeast of the spring mound. Eight study profiles are on the western margin of the Cottonwood Canyon floodplain and are ~3 km south of the Cienega Amarilla spring mound (Figs. 1 and 2b). Supplementary Table 1 contains geographic coordinates of Cienega Amarilla and Cottonwood Canyon profiles. Profile descriptions included sediment texture, color, pedogenic alteration, and stratigraphic boundaries. Stratigraphic units were differentiated based on lithology and/or bounding discontinuities often demarcated by buried soils. These units were correlated spatially via physical tracing, lithostratigraphic characteristics, radiocarbon ages, and temporally diagnostic archaeological artifacts. Samples collected for laboratory analysis and dating included sediment, plant macrofossils, mollusks, and archaeological artifacts.

Forty-four accelerator mass spectrometry (AMS) ^{14}C ages, augmented by temporally diagnostic prehistoric ceramics, provide age control for the alluvial sequences. Prior to destructive ^{14}C dating at the National Science Foundation Arizona Accelerator Mass Spectrometry Laboratory, the macrobotanical samples were identified to genus or species level. Short-lived plant parts (e.g., seeds, stems, and twigs) were preferentially selected, including material from archaeological features (e.g., hearths and roasting pits) and detrital macrofossils from non-archaeological contexts. ^{14}C pretreatment of both charred and uncharred plant macrofossils followed the standard acid–base–acid protocol. Pretreatment of gastropod shells involved

https://doi.org/10.1017/qua.2016.14 Published online by Cambridge University Press

sonication in first milli-Q water and then 3% H_2O_2, followed by multiple milli-Q water rinses. Radiocarbon ages presented in the text were calibrated using the OxCal v. 4.2 program (Ramsey, 2009) utilizing IntCal2013 (Reimer et al., 2013), with uncertainties given at the 2-sigma confidence level.

Ten pollen samples from Cienega Amarilla, including two modern surface samples and eight subsurface samples collected from arroyo wall exposures, were processed and analyzed using methods detailed in Smith (1998). Past floodplain vegetation in the spring mound vicinity was inferred by comparing fossil pollen assemblages to modern surface samples from (1) a wetland area within the entrenched modern arroyo channel and (2) the more xeric valley floor terrace. Two Cienega Amarilla sediment samples were processed for mollusks, ostracodes, and algae using procedures detailed in Forester (1988) and Palacios-Fest (1994).

Select sediment and soil samples were analyzed for organic carbon content using the dichromate (Walkley-Black) method (Janitzky, 1986), calcium carbonate content using gas manometry with a Chittick apparatus (Machette, 1986), and gypsum content using the gypsum–bassanite phase change method (Lebron et al., 2009). Initial organic carbon results were multiplied by 1.33 to correct for the systematic incomplete digestion (~76%) of the organic matter (Walkley and Black, 1934; Schumacher, 2002).

The isotopic (δD and $\delta^{18}O$) composition of water collected from a Cienega Amarilla spring pool was analyzed on a gas-source isotope ratio mass spectrometer (Finnigan Delta S) at the University of Arizona Environmental Isotope Laboratory. Standardization is based on Vienna Standard Mean Ocean Water (VSMOW) and Standard Light Antarctic Precipitation (SLAP) international reference materials.

ALLUVIAL STRATIGRAPHY AND GEOCHRONOLOGY

Six stratigraphic units identified at the study exposures were designated Roman numerals I–VI from oldest to youngest. Stratigraphic profiles at Cienega Amarilla and Cottonwood Canyon are illustrated in Figures 3 and 4, respectively. Supplementary Table 2 contains detailed field descriptions. AMS ^{14}C dates (Table 1) are discussed as calibrated, 2-sigma ranges in cal yr BP expressed as the median age $\pm 2\sigma$, rounded to the nearest decade. Figure 5 depicts the inferred chronological framework. Soil chemistry results are presented in Figure 6 and Supplementary Table 3. Figure 7 contains pollen analysis results, Supplementary Table 4 contains pollen data, and Supplementary Table 5 summarizes plant macrofossil data. Table 2 contains mollusk and ostracode results.

Stratum I

Exposed at only two Cienega Amarilla profiles, stratum I is ~1.5 m thick and consists of gray silty clay alluvium that caps sandstone bedrock (Fig. 8). Stratum I soil formation is weak, consisting of an ABb horizon with strong angular blocky ped structure and slightly elevated organic carbon content. Plant macrofossils consist mostly of juniper and cottonwood/willow charred wood, including a fragment that provided a ^{14}C age of 3740 ± 90 cal yr BP (AA-95501). Lacking bulrush or cattail pollen grains, stratum I pollen resembles the modern terrace assemblage, and the dominant Cheno-am (*Chenopodium* and *Amaranthus*) signal is attributed primarily to four-wing saltbush.

Stratum I at Cottonwood Canyon consists of >2 m of sandy mud overprinted with a weakly developed soil (Btjkb horizon) with subangular blocky ped structure, carbonate filaments, and minor illuvial clay. Coarser and less organic-rich than correlative stratum I deposits at Cienega Amarilla, Cottonwood Canyon stratum I represents a better drained and slightly higher energy fluvial environment. ^{14}C-dated juniper charcoal from an archaeological thermal feature at its upper contact suggests that stratum I deposition at Cottonwood Canyon ended before 3590 ± 90 cal yr BP (AA-95506).

Stratum II

Stratum II consists of a 2- to 4.5-m-thick package of sandy stream alluvium with interbedded mud layers. It is present at Cienega Amarilla in exposures deeper than ~4 m but absent at Cottonwood Canyon. Where not erosionally truncated, the upper meter of stratum II contains a weak soil profile with ABkjb-Bwb horizonation. Some of the deeper, clay-rich beds are laminated, and others show evidence of incipient pedogenesis implying episodic deposition. Detrital plant remains are dominated by charred wood from juniper, piñon pine (*Pinus edulis*), cottonwood/willow, and greasewood (*Sarcobatus* sp.). Bulrush achenes (fruits) and possible common reed (*Phragmites* sp.) stems are locally present. Three radiocarbon ages associated with stratum II range from 2610 ± 120 cal yr BP (AA-97644) near its base to 2540 ± 190 cal yr BP (AA-100899) at its top and suggest rapid deposition. Compared with stratum I, stratum II pollen concentrations exhibit decreased Cheno-ams, increased grasses, and the appearance of sagebrush (*Artemisia* sp.) and bulrush. Succineidae (small, semiaquatic gastropods) shells are scattered throughout stratum II.

Stratum III

Stratum III is typically ~3 m thick at Cienega Amarilla, where tufa and marl facies dominate the spring mound area and clay-rich paludal (marsh) facies dominate the surrounding floodplain. Correlative Cottonwood Canyon deposits are generally thinner and consist entirely of fluvial deposits. Stratum III was divided into three subunits—IIIa, IIIb, and IIIc—to simplify its description and interpretation.

IIIa

At Cienega Amarilla, stratum IIIa is a ~0.1- to 1.0-m-thick fluvial deposit of sand or muddy sand. It is a distinct marker horizon identifiable at most Cienega Amarilla

https://doi.org/10.1017/qua.2016.14 Published online by Cambridge University Press

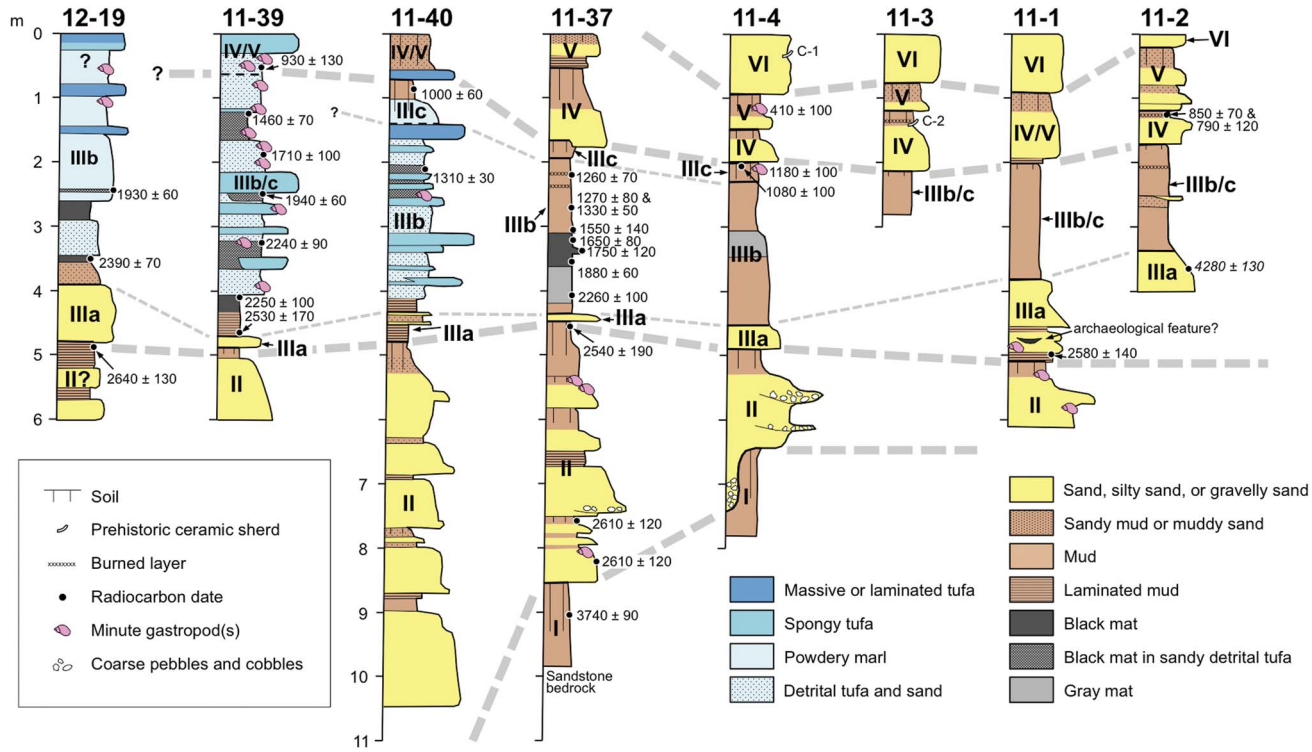

Figure 3. (color online) Cienega Amarilla stratigraphic sections. C-1 is an undifferentiated Cibola White Ware sherd (AD 650–1325), and C-2 is an early Cibola White Ware sherd with sand temper (AD 800–1000). Radiocarbon dates are 2-sigma ranges in cal yr BP expressed as the median age ± 2σ, rounded to the nearest decade. Age in italics was rejected as anomalously old for context, and sample is probably redeposited. See web version of article for color version of this figure that differentiates groundwater carbonate facies.

profiles (Fig. 8). At Cottonwood Canyon, stratum IIIa is 0.3–1.7+ m thick, consists of sand with pebble lenses, and is separated from stratum I by an erosional contact. Taxa represented by plant macrofossils are similar to stratum II except that cottonwood/willow is absent. ^{14}C dates on charred twigs from immediately below and above IIIa at

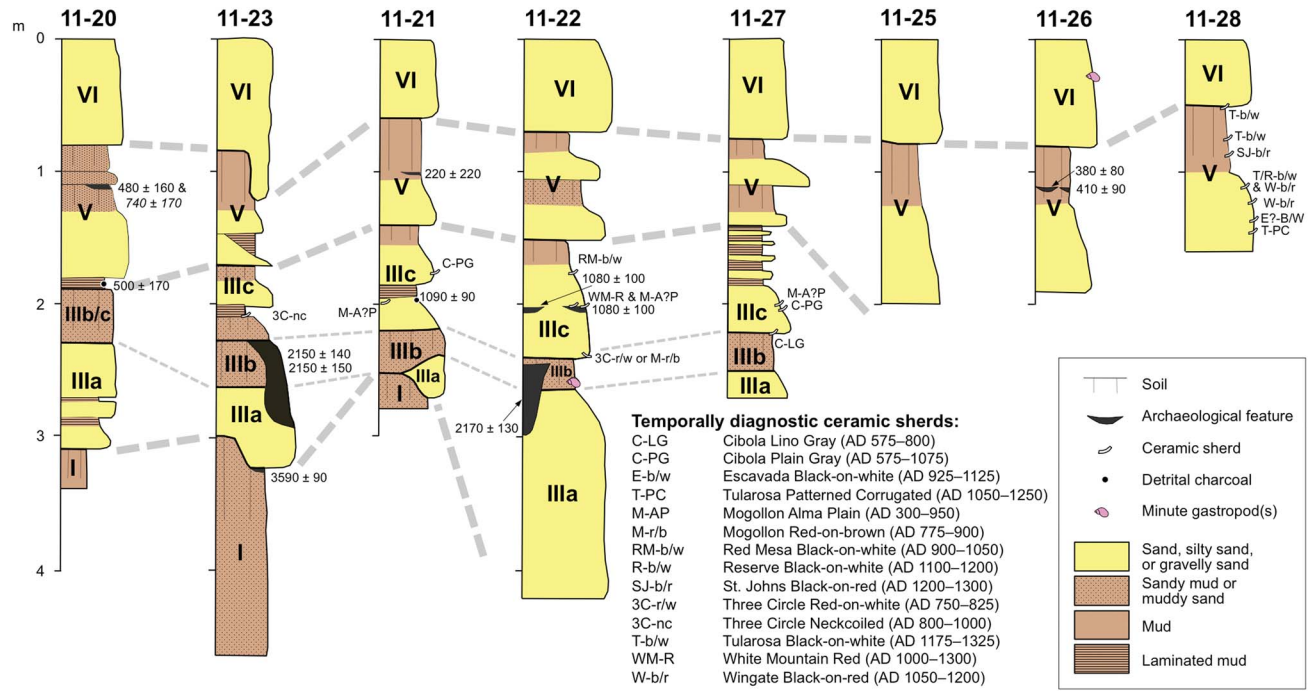

Figure 4. (color online) Cottonwood Canyon stratigraphic sections. Radiocarbon dates are 2-sigma ranges in cal yr BP expressed as the median age ± 2σ, rounded to the nearest decade. Age in italics was rejected as anomalously old for context, and sample is probably old wood.

https://doi.org/10.1017/qua.2016.14 Published online by Cambridge University Press

Table 1. Accelerator mass spectrometry radiocarbon dates and $\delta^{13}C$ values from Cienega Amarilla and Cottonwood Canyon.

Lab number	Unit	Profile	Depth (m)	Material dated	$\delta^{13}C$ (PDB)[a]	^{14}C age ± 1σ (^{14}C yr BP)[b]	2σ calibrated age range (cal yr BP)[c]	Median age ± 2σ (cal yr BP)[d]
Cienega Amarilla (n = 31)								
AA-99240	V	11-4, G-2	0.84	Succineidae shell	–1.2	387 ± 30*	509–319	410 ± 100
AA-95503	IV	11-2, R-4	1.19–1.21	Charred *Poaceae* stems	–11.3	830 ± 70	910–670	790 ± 120
AA-100898	IV	11-2, R-4	1.19–1.21	Charred *Poaceae* stems	–11.9	929 ± 27*	920–789	850 ± 70
AA-101881	IV	11-39, R-11	0.45–0.50	Uncharred *Scirpus* achenes (4), unidentified seeds (7), and stems (7)	–22.2	1020 ± 60	1060–800	930 ± 130
AA-105541	IIIc	11-40	0.7–1.0	Organic-rich sediment (A horizon)	–21.0	1085 ± 18*	1054–938	1000 ± 60
AA-95627	IIIc	11-4, R-4	1.71–1.75	Charred *Juniperus* wood	–20.1	1145 ± 29*	1174–976	1080 ± 100
AA-99239	IIIc	11-4, G-1	1.75–1.79	Succineidae shells (3)	–0.4	1252 ± 26*	1275–1084	1180 ± 100
AA-99219	$IIIb_4$	11-37, R-17	2.15	Charred *Juniperus* wood	–20.6	1357 ± 27*	1325–1188	1260 ± 70
AA-104619	$IIIb_3$	11-37, R-18	2.65–2.7	Uncharred *Scirpus* achenes (20)	–23.7	1372 ± 38*	1352–1187	1270 ± 80
AA-101882	IIIb	11-40, R-1	2.05–2.1	Uncharred *Scirpus* achenes (10)	–24.1	1380 ± 26*	1339–1275	1310 ± 30
AA-97647	$IIIb_3$	11-37, R-18	2.65–2.7	Uncharred *Scirpus* achenes (10)	–25.2	1417 ± 36	1380–1285	1330 ± 50
AA-99202	IIIb	11-39, R-12	1.21–1.26	Uncharred *Scirpus* achenes (10)	–24.0	1557 ± 27*	1527–1390	1460 ± 70
AA-100483	$IIIb_3$	11-37	3.0–3.1	Uncharred *Scirpus* achenes (12)	–24.2	1614 ± 25*	1690–1415	1550 ± 140
AA-95499	$IIIb_2$	11-37	3.2	Uncharred *Scirpus* achenes (8)	–24.2	1759 ± 25*	1734–1571	1650 ± 80
AA-104620	IIIb	11-39, R-10	1.85–1.9	Uncharred *Scirpus* achenes (22)	–24.5	1769 ± 25*	1807–1607	1710 ± 100
AA-97643	$IIIb_2$	11-37, R-19	3.3–3.4	Uncharred *Scirpus* achenes (10)	–24.2	1833 ± 36	1870–1634	1750 ± 120
AA-102662	$IIIb_2$	11-37	3.6–3.7	Uncharred unknown stem fragments (20)	–19.4	1934 ± 29*	1946–1821	1880 ± 60
AA-101884	IIIb	12-19, R-4	2.43–2.46	Uncharred *Scirpus* achenes (10)	–23.5	1963 ± 26*	1989–1865	1930 ± 60
AA-101880	IIIb	11-39, R-9	2.47–2.5	Uncharred *Scirpus* achenes (11)	–23.9	2002 ± 26*	2000–1889	1940 ± 60
AA-101879	IIIb	11-39, R-8	3.22–3.27	Uncharred *Scirpus* achenes (10)	–25.1	2210 ± 32	2325–2147	2240 ± 90
AA-99201	IIIb	11-39, R-6	4.05–4.1	Uncharred *Scirpus* achenes (10)	–25.6	2272 ± 30*	2350–2159	2250 ± 100
AA-102033	$IIIb_1$	11-37	4.0–4.1	Charred grass? stems (33)	–19.0	2277 ± 36	2352–2158	2260 ± 100
AA-102672	IIIb	12-19, R-2	3.45–3.55	Uncharred *Scirpus* achenes (30)	–25.1	2350 ± 30*	2464–2324	2390 ± 70
AA-100899	II	11-37, R-23	4.45–4.6	Charred *Populus/Salix* twig	–26.1	2430 ± 80	2720–2350	2540 ± 190
AA-100482	IIIb	11-39, R-5	4.65–4.7	Charred *Atriplex* twig	–11.6	2452 ± 29*	2704–2361	2530 ± 170
AA-95502	IIIa	11-1, feature?	4.92–5.02	Charred unknown nutshells	–21.8	2475 ± 26*	2719–2434	2580 ± 140
AA-97646	II	11-37, R-12	7.58	Charred monocotyledon tissue	–11.4	2501 ± 23*	2727–2490	2610 ± 120
AA-97644	II	11-37, R-6	8.12–8.2	Charred *Sarcobatus* twig (w/<5 rings)	–24.3	2506 ± 24*	2735–2490	2610 ± 120
AA-101883	II?	12-19, R-1	4.8–4.82	Uncharred *Scirpus* achenes (7)	–25.4	2577 ± 32*	2762–2510	2640 ± 130
AA-95501	I	11-37, R-2	9.0	Charred *Populus/Salix* wood	–25.6	3480 ± 28*	3835–3648	3740 ± 90
AA-95500	IIIa	11-2, R-1	3.55–3.65	Charred monocotyledon tissue	–23.5	3848 ± 27[e]	4407–4155	4280 ± 130
Cottonwood Canyon (n = 13)								
AA-100542	V	11-21, Feat. 3[f]	1.0–1.01	Charred *Picea*? needle, *Poaceae* stem, and *Atriplex* fruit core	–15.7	210 ± 60*	430–0	220 ± 220
AA-99220	V	11-26, Feat. 12[g]	1.1–1.15	Charred unknown twig and disseminules (2)	–23.6	308 ± 30*	464–300	380 ± 80
AA-95508	V	11-26, Feat. 13[g]	1.12–1.17	Charred *Atriplex* utricle cores (6)	–10.9	365 ± 22*	498–319	410 ± 90
AA-99198	V	11-20, Feat. 1[f]	1.1–1.18	Charred *Physalis* seeds (3), unknown seed, *Pinus* twig (w/5 rings)	–18.3	460 ± 70	640–320	480 ± 160
AA-95505	V	11-20, R-6[f]	1.84	Charred *Juniperus* twig (w/2 rings)	–20.1	530 ± 80	670–330	500 ± 170
AA-95504	V	11-20, Feat. 1[f]	1.1–1.18	Charred *Juniperus* wood	–22.4	780 ± 60[e]	900–570	740 ± 170
AA-100480	IIIc	11-22, Feat. 9[f]	1.7–1.77	Charred *Zea mays* kernel	–9.3	1149 ± 37*	1176–976	1080 ± 100
AA-100481	IIIc	11-22, Feat. 11[f]	1.37–1.42	Charred *Zea mays* kernel	–8.7	1164 ± 28*	1178–986	1080 ± 100
AA-95629	IIIc	11-21, R-1[f]	1.95–1.99	Charred *Zea mays* cupule	–10.0	1178 ± 29*	1181–997	1090 ± 90
AA-95507	IIIb/IIIc	11-23, Feat. 4[f]	2.7–3.0	Charred *Atriplex* wood	–9.9	2128 ± 21*	2291–2010	2150 ± 140
AA-101878	IIIb	11-22, Feat. 5[f]	2.3–2.4	Charred *Atriplex* wood	–10.1	2138 ± 21*	2299–2040	2170 ± 130
AA-93782	IIIb/IIIc	11-23, Feat. 4[f]	2.7–3.0	Charred *Zea mays* cupules (3)	–10.5	2140 ± 36	2304–2002	2150 ± 150
AA-95506	I/IIIa	11-23, Feat. 6[f]	3.34–3.4	Charred *Juniperus* wood	–21.0	3350 ± 23*	3683–3498	3590 ± 90

Note: Asterisk (*) indicates high-precision analysis (multiple spectrometer targets).
[a]Pee Dee Belemnite reference standard.
[b]Radiocarbon ages are corrected for carbon-isotope fractionation, and standard deviations are given at 1-sigma.
[c]Radiocarbon ages were calibrated using the OxCal v. 4.2 program (Ramsey, 2009) utilizing IntCal2013 (Reimer et al., 2013).
[d]Simple median of the 2σ calendar range with error being one-half the calendar range, both rounded to nearest decade.
[e]Rejected age that is anomalously old for context (old wood or redeposited).
[f]Site LA170848.
[g]Site LA170847.

Cienega Amarilla bracket the age of stratum IIIa between 2540 ± 190 (AA-100899) and 2530 ± 170 cal yr BP (AA-100482), and a charred nutshell within IIIa has a ^{14}C age of 2580 ± 140 cal yr BP (AA-95502). Stratum IIIa might represent a single storm, although a possible archaeological thermal feature within this unit at Cienega Amarilla suggests it represents multiple precipitation events over at least several decades or, at most, a few centuries.

IIIb

At the Cienega Amarilla spring mound, stratum IIIb is dominated by groundwater carbonate facies (Fig. 9). Tufa layers that formed in situ are typically <30 cm thick and consist primarily of spongy tufa with vertically oriented voids that formed around reedy vegetation. Some of the tufa strata, however, are dense and laminar flowstones or powdery

https://doi.org/10.1017/qua.2016.14 Published online by Cambridge University Press

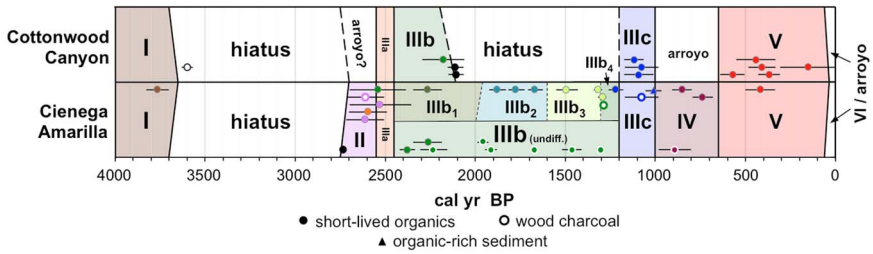

Figure 5. (color online) Geochronology of Cienega Amarilla and Cottonwood Canyon areas. Radiocarbon dates are calibrated ages plotted with 1-sigma standard deviation bars. Two rejected dates (see Table 1) are excluded. See web version of article for color version of this figure that depicts stratigraphic context of individual dates and shows dates associated with groundwater carbonate facies outlined in white.

wetland marls. Tufa deposition at the spring mound began shortly after 2250 ± 100 cal yr BP (AA-99201) and accumulated at a rapid rate until 1460 ± 70 cal yr BP (AA-99202). Uncharred bulrush achenes and stems tentatively identified as bulrush are abundant. Gastropods and ostracodes from IIIb spring mound deposits dating 2240 ± 90 cal yr BP

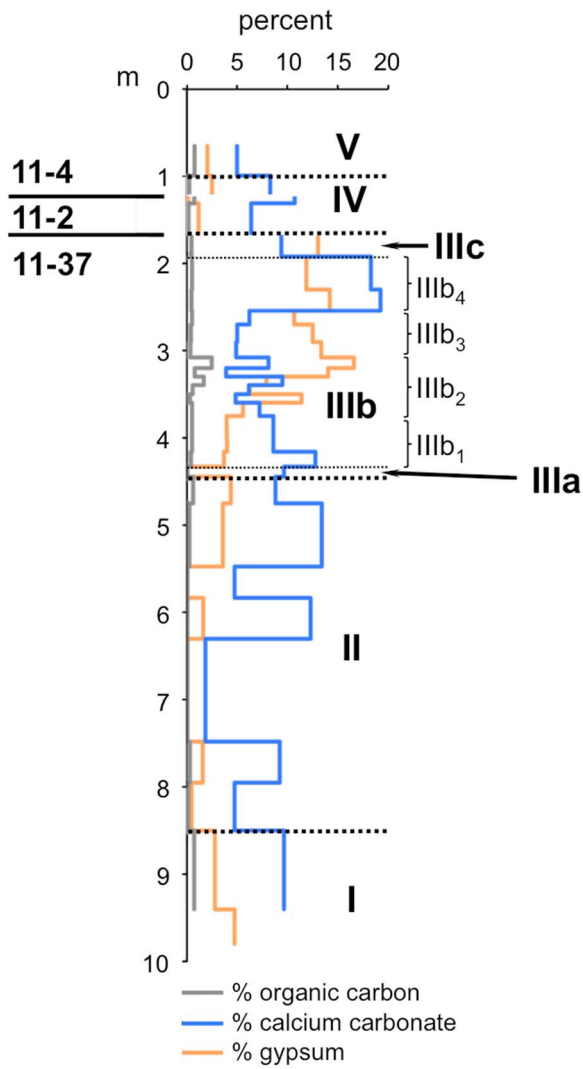

Figure 6. (color online) Cienega Amarilla soil geochemistry at profiles 11-4, 11-2, and 11-37.

(AA-101879) include a variety of types, including aquatic, semiaquatic, and terrestrial species (Table 2). The groundwater carbonate layers are interbedded with very thinly bedded alluvium composed of sand and tufa rip-up clasts. Many of the alluvial beds are black mats darkened by organic-rich sediment containing plant macrofossils, including some partially decomposed stems (bulrush?) still oriented in upright growth positions suggestive of burial by rapid, episodic deposition.

Stratum IIIb floodplain deposits surrounding the Cienega Amarilla spring mound are dominated by clay-rich, marsh facies. Stratum IIIb was examined in detail only at profile 11-37 where a fresh exposure could be safely accessed. Here, IIIb was further subdivided into $IIIb_1$–$IIIb_4$ to facilitate discussion (Fig. 8).

Substratum $IIIb_1$ comprises the basal ~50 cm of stratum IIIb and consists of gray, clay-rich deposits. Charred stems from 20 cm above the slightly oxidized base of $IIIb_1$ at profile 11-37 yielded an age of 2260 ± 100 cal yr BP (AA-102033), but a 2530 ± 170 cal yr BP (AA-100482) age on a charred saltbush twig from the base of clay-rich IIIb deposits beneath the carbonate spring mound suggests IIIb deposition at Cienega Amarilla began earlier. Above $IIIb_1$ is a ~60-cm-thick, thinly bedded, organic-rich "black mat" ($IIIb_2$). Radiocarbon dates on plant macrofossils indicate that the $IIIb_2$ black mat formed between 1880 ± 60 cal yr BP (AA-102662) and 1650 ± 80 cal yr BP (AA-95499), with the most organic-rich portion dating prior to 1750 ± 120 cal yr BP (AA-97643). Identifiable plant remains in $IIIb_2$ consist mostly of abundant bulrush achenes and pollen indicative of emergent aquatic vegetation. Ubiquitous stem fragments are degraded and too poorly preserved to be identified on the basis of anatomy. Their abundance and direct association with bulrush achenes (fruit), however, circumstantially suggest that these stems might also represent bulrush plants. Faunal remains include snail and ostracode species indicative of marshy conditions (Table 2). From the base of $IIIb_1$ to the sharp upper boundary of the $IIIb_2$ black mat, trends of decreasing calcium carbonate (~13%–4%), increasing gypsum (~4%–17%), and increasing organic carbon (0.4%–2.4%) content are evident. Gypsum occurs as tiny clumps of intergrown lathe crystals, whereas carbonate occurs as small soft masses.

The $IIIb_2$ black mat is capped by a ~50-cm-thick, light-olive-gray layer ($IIIb_3$) of very thinly bedded clay with high

https://doi.org/10.1017/qua.2016.14 Published online by Cambridge University Press

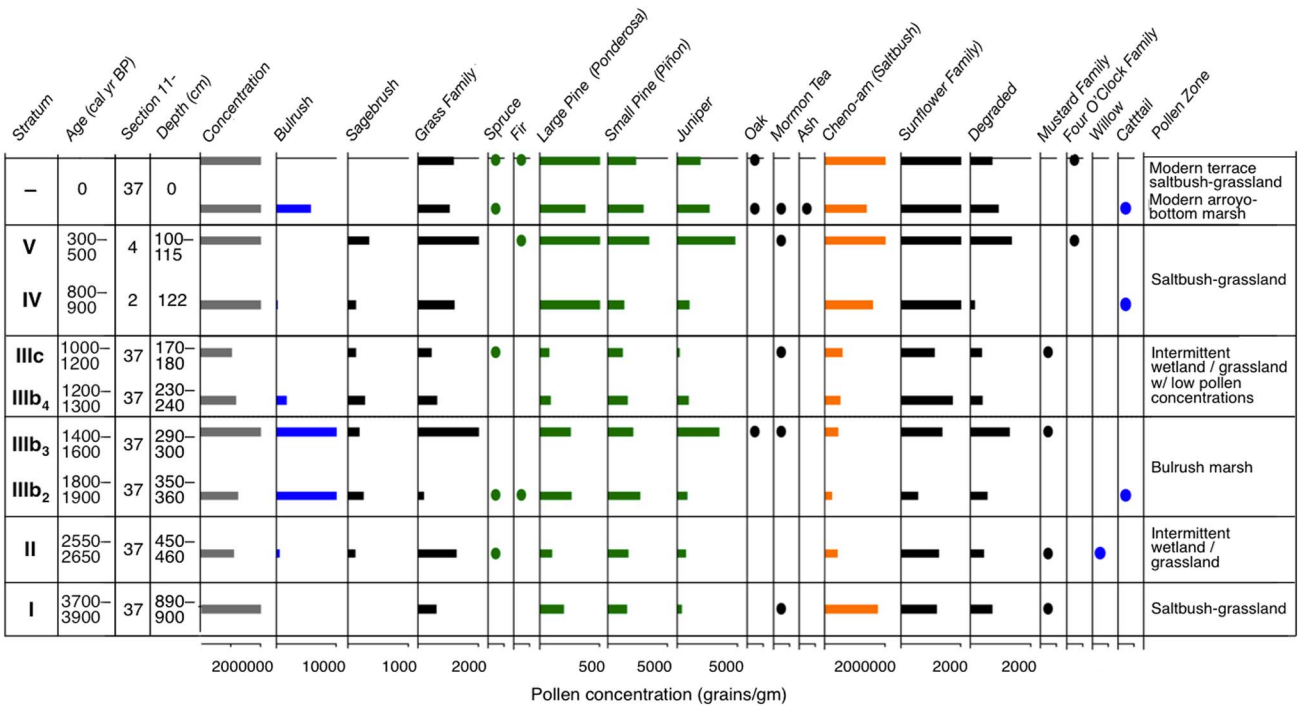

Figure 7. (color online) Cienega Amarilla pollen analysis results showing pollen concentrations in grains per gram. Oval symbols indicate presence. Supplementary Table 4 contains raw data and additional details.

gypsum content (~11%–13%) but substantially less organics (0.3%–0.5%) than $IIIb_2$. The gypsum deposits precipitated from shallow (1–2 m deep), brackish groundwater wicked to the surface by evaporation (Quade et al., 2008). Although this horizon's color and texture resemble wetland marl deposits (cf. Pigati et al., 2014), its carbonate content is relatively low (~5%–6%). In contrast to the underlying black mat, plant macrofossils are less plentiful in $IIIb_3$. Uncharred bulrush achenes from $IIIb_3$'s base produced a ^{14}C date of 1550 ± 140 cal yr BP (AA-100483) and from its top yielded ages of 1330 ± 50 and 1270 ± 80 cal yr BP (AA-97647 and -104619). Pollen continues to be dominated by bulrush, but more grains are degraded, and more nonaquatic plant types are represented, including a significant increase in grass, juniper, and sunflower family.

Substratum $IIIb_4$ forms the upper part of IIIb floodplain deposits and consists of pinkish-gray clay with peak carbonate (~19%) and continued high gypsum (~12%–14%) content. Very thin, wispy bands darkened by fine charcoal probably represent charcoal washed onto the floodplain after wildfires burned the adjacent hillslopes. Charred juniper wood from one of the dark bands provided an age of 1260 ± 70 cal yr BP (AA-99219). Stratum $IIIb_4$ is characterized by substantially decreased amounts of grass, bulrush, and juniper pollen. Lower overall pollen concentrations in this horizon may reflect lower density vegetation or rapid deposition.

At Cottonwood Canyon, stratum IIIb consists of a 20- to 40-cm-thick layer of muddy sand alluvium with a weakly developed soil expressed as a Bwb horizon. The presence of a Succineidae shell might suggest moist surface conditions, although it is possible this isolated shell was reworked from older deposits. Stratum IIIb contains cultural deposits associated with a buried site (LA170848). Charred saltbush wood and maize cupules (cob pockets that held two kernels) from archaeological features at or near the IIIb upper contact provided ages of 2150 ± 140, 2150 ± 150, and 2170 ± 130 cal yr BP (AA-95507, -93782, and -101878), indicating that IIIb deposition at Cottonwood Canyon ended by ~2100 cal yr BP.

IIIc

At Cienega Amarilla, stratum IIIc typically consists of a thin cumulic soil formed in grayish-brown clay (Fig. 8). Most commonly, this soil is expressed as an ABsskyb horizon with slickensides and gypsum and carbonate precipitates. Three ^{14}C dates from IIIc contexts range from 1180 ± 100 (AA-99239; Succineidae shells) to 1000 ± 60 cal yr BP (AA-105541; organic-rich sediment). The IIIc pollen record is nearly identical to that of $IIIb_4$, except that bulrush pollen drops out completely. Plant macrofossils are limited to juniper and oak (*Quercus* sp.) wood. Succineidae shells are locally common in Cienega Amarilla IIIc deposits.

At Cottonwood Canyon, IIIc consists of alternating layers of sand and mud. A Bwb soil horizon formed in the uppermost mud layer. Temporally diagnostic prehistoric ceramics sherds at the IIIb–IIIc contact at archaeological site LA170848 suggest that IIIc deposition at Cottonwood Canyon began after AD 800, after a millennium-long hiatus (Fig. 4). Charred maize kernels and cupules from archaeological deposits in IIIc yielded clustered ^{14}C ages of 1090 ± 90 (AA-95629) and 1080 ± 100 cal yr BP (AA-100480 and -100481).

https://doi.org/10.1017/qua.2016.14 Published online by Cambridge University Press

Table 2. Fossil mollusks and ostracodes at Cienega Amarilla and Cottonwood Canyon.

Taxon	Stratigraphic units and number of individuals recovered		Ecological preferences
	Cienega Amarilla	Cottonwood Canyon	
Mollusks			
Succineidae	II (5) IIIa (1) IIIc (15+) V (1)	IIIb (1)	Terrestrial; moist ground next to permanent water (Pigati et al., 2004)
Oreohelix houghi	–	VI (1)	Terrestrial
Physella virgata	$IIIb_2$ (4)[a]	–	Semiaquatic; wet meadows; can tolerate poorly oxygenated, standing water (Palacios-Fest, 2010; Pigati et al., 2014)
Fossaria parva	IIIb (1)[b]	–	Semiaquatic (terrestrial during warm months, aquatic during cold months); permanent or ephemeral streams, lakes, ponds; lotic or lentic (Evanoff, 1987)
Pyrgulopsis sp.	IIIb (1)[b]	–	Aquatic; permanent springs, streams, rivers; commonly known as "springsnails"; benthic; generally concentrated near spring sources (Hershler and Sada, 2002)
Ferrissia hendersoni	IIIb (1)[b]	–	Aquatic; permanent, lakes, ponds, streams; lotic (Basch, 1963; Palacios-Fest, 2010)
Pisidium casertanum	IIIb (2)[b]	–	Aquatic; permanent, streams, lakes, ponds; lotic (Palacios-Fest, 2010)
Gastrocopta tappaniana	IIIb (1)[b]	–	Terrestrial; wet to moist, calcareous soils (Evanoff, 1987)
Ostracodes		–	
Chlamydotheca arcuata	IIIb (10)[b]	–	Permanent springs, streams, marshes, lake margins; tropical species that cannot survive water temperatures <20°C (thermal springs or summer occurrences) (Forester, 1991)
Ilyocypris bradyi	$IIIb_2$ (11)[a] IIIb (20)[b]	–	Permanent or ephemeral streams, lakes, ponds; marshes with persistent, lotic surface water; high water table and spring discharge (Palacios-Fest, 2010; Pigati et al., 2014)
Cypria ophthalmica	IIIb (22)[b]	–	Permanent lakes, ponds; high water table and spring discharge (Palacios-Fest, 2010)
Cypridopsis okeechobei	IIIb (226)[b]	–	Permanent springs, streams, lakes; thermally and chemically stable conditions; most abundant in spring pools near spring orifices (Pigati et al., 2014)
Microdarwinula sp.	IIIb (44)[b]	–	Aquifers (Karanovic, 2012)

[a]Extracted from 100 g of ~1900–1800 cal yr BP sediment from profile 11-37, 3.4–3.6 m below surface.
[b]Extracted from 100 g of ~2300–2200 cal yr BP sediment from profile 11-39, 3.22–3.47 m below surface.

Stratum IV

At Cienega Amarilla, stratum IV is ~50–70 cm thick and consists of fluvial sand overlain by mud. A weakly developed soil with ABb-Bwkb horizonation formed at the top of stratum IV in the mud layer. A distinct, 1- to 2-cm-thick layer of burned C_4 (inferred from $\delta^{13}C$ values) grass stems within the mud layer provided ^{14}C ages of 850 ± 70 and 790 ± 120 cal yr BP (AA-100898 and -95503). An early Cibola White Ware ceramic sherd at the bottom of the burned layer implies the lower (sandy) portion of IV predates AD 1000. Short-lived plant macrofossils including a few bulrush achenes in stratum IV tufa deposits yielded an age of 930 ± 130 cal yr BP (AA-101881). Palynological evidence suggests saltbush-grassland vegetation, but traces of bulrush and cattail pollen indicate nearby marshy areas.

Stratum IV is absent at Cottonwood Canyon, suggesting that stratum IV aggradation at Cienega Amarilla resulted from channel entrenchment in upvalley areas. Paleochannels noted in arroyo wall exposures south of the Cottonwood Canyon study profiles were conceivably formed during this erosional episode.

Stratum V

Stratum V is present at both Cienega Amarilla and Cottonwood Canyon. It is 0.5–1 m thick and consists primarily of sand overlain by grayish-brown mud in which an ABwb soil horizon formed. A Succineidae shell found within the Cienega Amarilla stratum V soil yielded an age of 410 ± 100 cal yr BP (AA-99240) and suggests moist surface conditions. At spring mound exposures, strata IV and V are indifferentiable, but ^{14}C dates suggest localized tufa deposition continued after ~1000 cal yr BP (Fig. 9). Cienega Amarilla stratum V pollen is similar to stratum IV pollen except that bulrush and cattail pollen is absent and plant macrofossils are limited to juniper wood.

Stratum V alluvium at Cottonwood Canyon probably includes sand and gravel paleochannel fills exposed in the modern arroyo walls south of the study profiles. Its age is secured by five ^{14}C dates ranging from 500 ± 170 cal yr BP to 220 ± 220 cal yr BP (AA-95505 and -100542) on short-lived plant macrofossils from archaeological features. At profile 11-28, stratum V contains ceramic sherds and other artifacts redeposited from a Pueblo II–III (AD 900–1300) period archaeological site (LA 170847) situated immediately upslope.

Stratum VI

At both Cienega Amarilla and Cottonwood Canyon, stratum VI is a 0.2- to 1.3-m-thick surface layer of bedded, fluvial sand. ^{14}C ages associated with underlying deposits suggest stratum VI is younger than ~200 cal yr BP. Stratum VI

https://doi.org/10.1017/qua.2016.14 Published online by Cambridge University Press

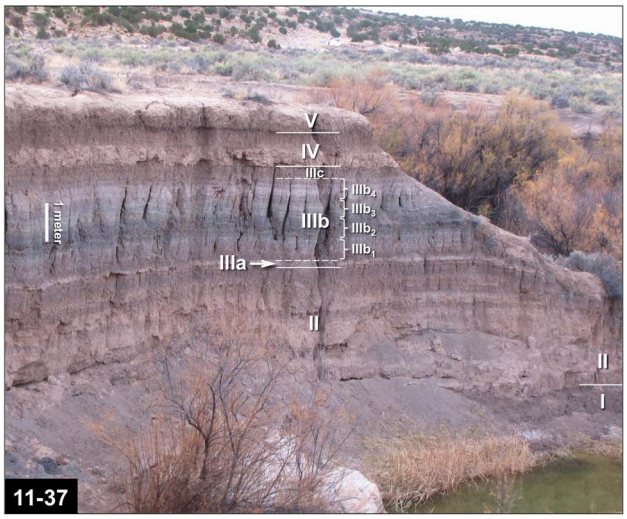

Figure 8. (color online) Arroyo exposure at Cienega Amarilla profile 11-37 showing unit IIIb subdivisions.

probably represents arroyo fan deposits associated with historical period stream entrenchment.

ISOTOPIC COMPOSITION OF SPRINGWATER

The δD and $\delta^{18}O$ values of a Cienega Amarilla springwater sample collected in October 2014 were compared to winter (October–April) and summer (May–September) precipitation isotope data from Global Network of Isotopes in Precipitation (GNIP) stations at Flagstaff (2137 m) and Tucson (753 m) (International Atomic Energy Agency and World Meteorological Organization, 2015). The elevation of Cienega Amarilla (1930 m) is intermediate between the Flagstaff and Tucson GNIP stations. Cienega Amarilla water isotope values fall between the average Flagstaff and Tucson winter values, suggesting that GWD at Cienega Amarilla is driven primarily by winter precipitation (Table 3, Fig. 10).

DISCUSSION

Geomorphic history

During the late Holocene, the Cienega Amarilla and Cottonwood Canyon floodplains underwent dramatic and rapid geomorphic changes, experiencing periods of rapid high-energy deposition, slow low-energy deposition, stability and soil formation, deep channel entrenchment and subsequent infilling, and carbonate spring mound and wetland formation. Many of these shifts appear to represent geomorphic and hydrologic responses to climate change and variability.

4000–2700 cal yr BP

The absence of middle and early Holocene deposits in study area exposures suggests erosion of older valley fills prior to ~4000 cal yr BP. This is consistent with arroyo formation 4900–4600 cal yr BP elsewhere in the Carrizo Wash watershed (Onken, 2015) and may correlate with widespread arroyo cutting ~4500 cal yr BP in southeastern Arizona (Waters and Haynes, 2001). Floodplain aggradation of fine-grained alluvium (stratum I) deposited by low-energy surface-runoff processes ~4000–3700 cal yr BP was followed by a depositional hiatus and floodplain stability until ~2700 cal yr BP (Figs. 4 and 11). Drought-tolerant

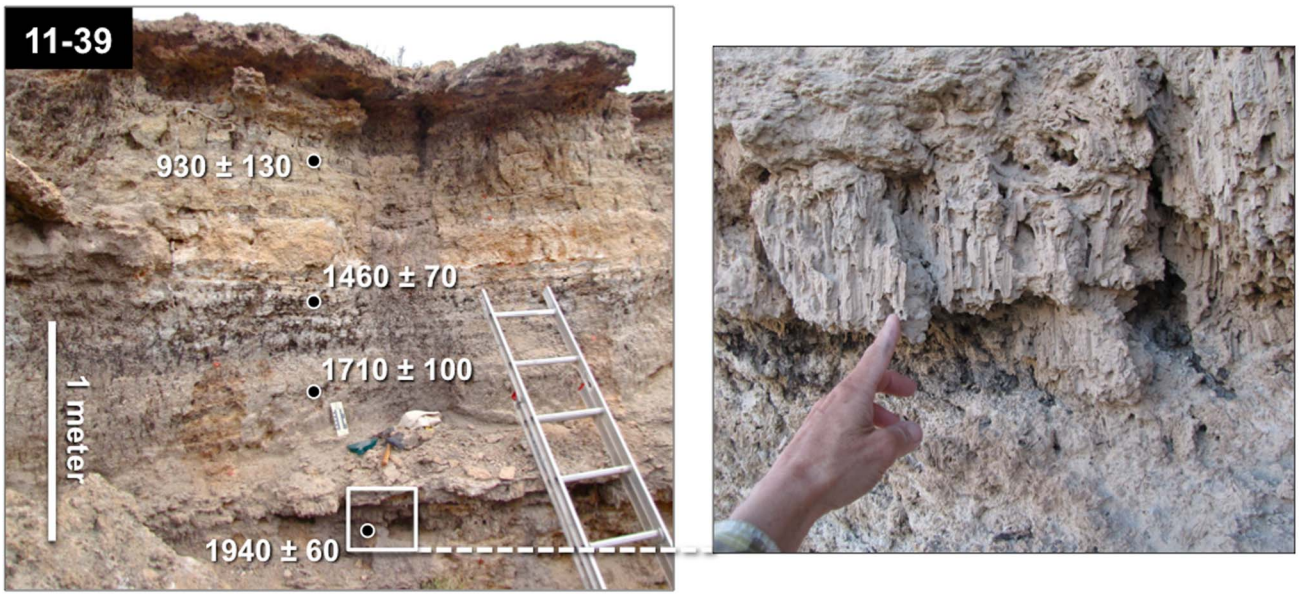

Figure 9. (color online) Groundwater carbonate and black mat deposits at profile 11-39 at Cienega Amarilla spring mound showing upper ~3 m of exposure (left) and a close-up of spongy tufa with vertically oriented voids that formed around reedy emergent aquatic vegetation immediately above the 1940 ± 60 cal yr BP date (right). Radiocarbon ages are 2-sigma ranges in cal yr BP expressed as the median age ± 2σ, rounded to the nearest decade.

https://doi.org/10.1017/qua.2016.14 Published online by Cambridge University Press

Table 3. Isotopic composition of Cienega Amarilla springwater (sample W63110) compared to winter (October–April) and summer (May–September) precipitation isotope data from GNIP (Global Network of Isotopes in Precipitation) stations at Flagstaff and Tucson, Arizona.

Location	Elevation (m amsl)	Latitude/longitude (decimal degrees)	Number of samples	$\delta^{18}O‰$	$\delta D‰$
Cienega Amarilla, NM	1930	34°25.518′N, 109°0.7218′W			
Springwater collected October 13, 2014, 11.5°C, 784 ppm total dissolved solids			1	−8.27 ± 0.09	−68.70 ± 0.9
Tucson, AZ (1981–2012)	753	32°14.166′N, 110°56.634′W			
Mean winter precipitation			158	−8.22 ± 3.10*	−54.20 ± 24.16*
Mean summer precipitation			98	−5.22 ± 2.83*	−37.93 ± 20.51*
Flagstaff, AZ (1961–1974)	2137	35°7.8′N, 111°40.2′W			
Mean winter precipitation			62	−9.74 ± 4.42*	−74.41 ± 29.18*
Mean summer precipitation			35	−5.03 ± 3.95*	−43.42 ± 23.90*

Notes: Asterisk (*) indicates calculated using data from International Atomic Energy Agency and World Meteorological Organization (2015). amsl, above mean sea level.

saltbush-grassland floodplain vegetation during this period suggests low water tables; four-wing saltbush—the most likely dominant species—is intolerant of high groundwater and late winter inundation (Ogle et al., 2012). The paleobotanical record indicates a minor component of emergent aquatic plants (bulrush) and phreatophyte trees (cottonwood/willow), suggesting localized marsh and riparian areas.

2700–2450 cal yr BP

Evidence of a major, ~2700–2550 cal yr BP pulse of alluvial deposition (stratum II) on the Cienega Amarilla floodplain is absent at Cottonwood Canyon (Figs. 3, 4 and 5). This implies either incision in one or both of the upvalley headwater reaches or upland erosion limited to the LA Draw/Agua Fria Creek catchment (Fig. 1). The latter explanation is more plausible because (1) no direct evidence of arroyo cutting during the 2700–2550 cal yr BP period was found at Cottonwood Canyon or elsewhere in the Carrizo Wash watershed, and (2) a locally major pulse of piedmont aggradation occurred ~20 km to the east during this interval (Onken, 2015), suggesting significant erosion of some upland mesa areas at this time.

Floodplain aggradation of braided distributary channel deposits (stratum II) at Cienega Amarilla ended by ~2550 cal yr BP. After a brief soil-forming period, aggradation resumed during the 2550–2450 cal yr BP interval, beginning with a pulse of sandy alluvium (stratum IIIa) deposited at both Cienega Amarilla and Cottonwood Canyon. Both the stratum II and IIIa alluvial pulses rapidly buried much of the pre-existing Cienega Amarilla floodplain vegetation, likely resulting in a wide, intermittently barren, braided channel covering much of the floodplain. Terrestrial gastropods

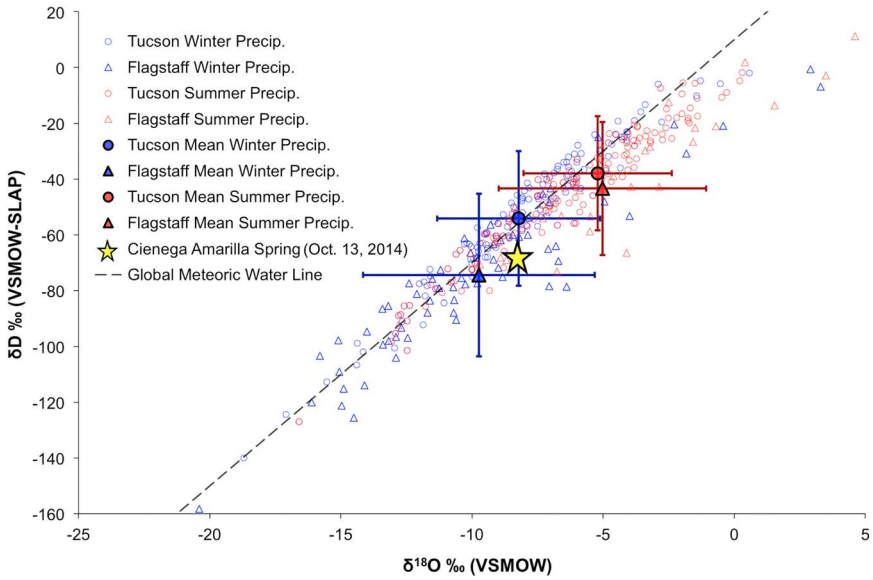

Figure 10. (color online) Isotopic composition of Cienega Amarilla springwater plotted relative to winter (October–April) and summer (May–September) precipitation isotope data from GNIP (Global Network of Isotopes in Precipitation) stations at Flagstaff and Tucson. Mean values are plotted with 1-sigma standard deviation bars. VSMOW, Vienna Standard Mean Ocean Water; SLAP, Standard Light Antarctic Precipitation.

https://doi.org/10.1017/qua.2016.14 Published online by Cambridge University Press

(Succineidae) in stratum II indicate moist surface soils and nearby permanent water (Pigati et al., 2004) (Table 2). Decreased saltbush and increased sagebrush pollen and greasewood macrofossils dating to the 2700–2450 cal yr BP interval (Fig. 7) suggest decreased summer and increased winter precipitation and a higher local water table. These changes, coupled with increased grass pollen concentrations and groundwater carbonate, imply a transition to moister, intermittent wet meadow floodplain conditions beginning ~2600 cal yr BP (Fig. 11).

2450–1600 cal yr BP

Cienega Amarilla floodplain aggradation from 2450 to 1600 cal yr BP slowed and was dominated by clay-rich GWD deposits (strata $IIIb_1$–$IIIb_2$) indicative of low-energy environments. Significant but localized wetland tufa deposition began ~2300 cal yr BP, resulting in the initial growth of the spring mound. Although mound growth probably continued until historical-period arroyo cutting, it appears most rapid from ~2300 to 1500 cal yr BP. Tufa and marl facies at the spring mound indicate spring orifice, spring pool, and marsh microenvironments associated with significant spring discharge. This implies a shift to groundwater-dominated floodplain processes and a substantial increase in effective moisture.

Snails in Cienega Amarilla tufa deposits dating ~2200 cal yr BP are mostly aquatic types (*Pisidium casertanum*, *Ferrissia hendersoni*, and *Pyrgulopsis* sp.) preferring ambient, lotic (flowing) waters and suggesting high spring discharge from a nearby spring orifice. Associated ostracodes are dominated by *Cypridopsis okeechobei*, a species that prefers thermally and chemically stable spring pool or orifice habitats (Forester and Smith, 1994; Pigati et al., 2010, 2014). The intermittent wet meadow ($IIIb_1$) surrounding the mound transitioned to marsh ($IIIb_2$) dominated by bulrush ~1900 cal yr BP, indicating increased surface water and spring discharge. The organic-rich marsh deposits contain semiaquatic *Physella virgata* snails and *Ilyocypris bradyi* ostracodes characteristic of persistent, lotic surface water in marsh habitats (Palacios-Fest, 2010; Pigati et al., 2014). Bulrush dominated the vegetation at both the spring mound and the surrounding marsh.

Although alluvial deposits at Cottonwood Canyon indicate lower energy environments during this period, floodplain processes there continued to be dominated by surface runoff. Deposition largely ended by ~2100 cal yr BP and was followed by an extended period of stable floodplain conditions and soil formation. These conditions are consistent with increased effective moisture, increased vegetation stabilizing hillslopes, and decreased runoff/sediment load.

1600–1200 cal yr BP

Cienega Amarilla spring mound growth slowed markedly ~1500 cal yr BP. Increased gypsum and carbonate precipitates in wetland deposits (upper $IIIb_2$, $IIIb_3$, and $IIIb_4$)

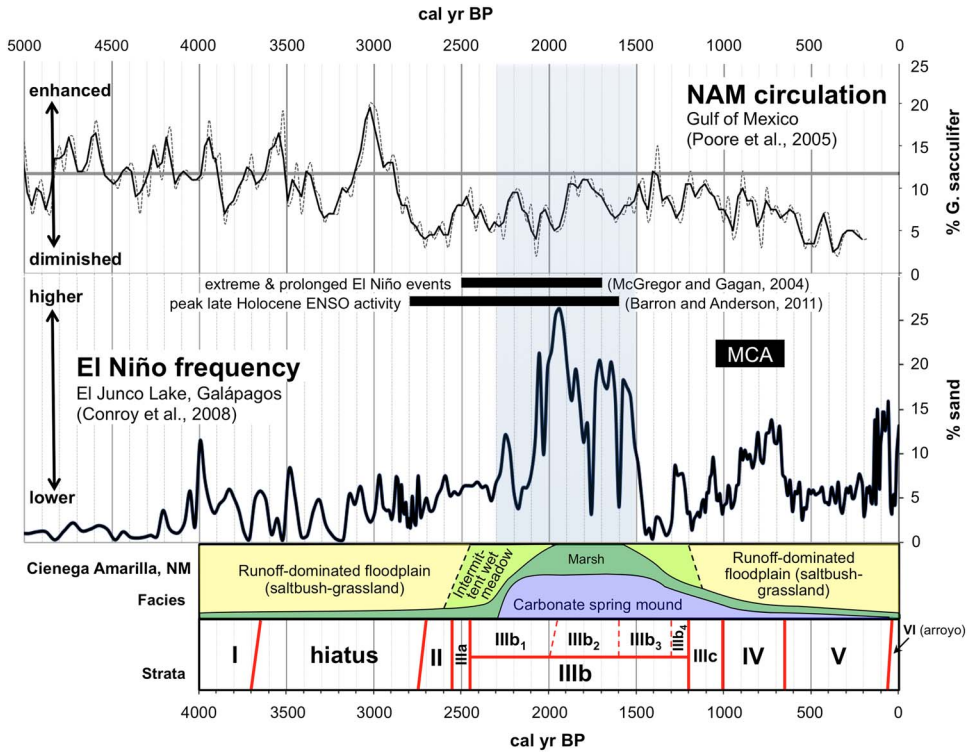

Figure 11. (color online) Cienega Amarilla chronology and reconstructed depositional facies with winter (El Niño) precipitation record from El Junco Lake (Conroy et al., 2008) and summer (North American monsoon) precipitation record from the Gulf of Mexico (Poore et al., 2005). The ~2300–1500 cal yr BP interval of maximum late Holocene groundwater discharge at Cienega Amarilla is shaded. ENSO, El Niño–Southern Oscillation; MCA, Medieval Climate Anomaly; NAM, North American monsoon.

https://doi.org/10.1017/qua.2016.14 Published online by Cambridge University Press

surrounding the spring mound imply drying of marshy areas caused by decreased GWD and a drop in the water table beginning between ~1600 and 1400 cal yr BP that drove capillary fringe zone soil water salts to saturation. Sulfur for gypsum formation was probably derived from sulfate-rich groundwater, which is common in the local region (Akers, 1964; Basabilvazo, 1997). The Supai Formation contains highly mineralized water containing salts including gypsum and carbonate, which enter the overlying aquifers by upward leakage (Akers, 1964). Although the pollen record suggests that emergent aquatic plants continued to dominate floodplain vegetation during the early part of the 1600–1200 cal yr BP period, by ~1300 cal yr BP bulrush was substantially reduced, and marshy areas were largely replaced by intermittent wet meadows dominated by grasses and composites. Thin, charcoal-rich zones deposited ~1350–1250 cal yr BP suggest burning of nearby slopes that coincides with a dry period ~1350 cal yr BP indicated by the nearby El Malpais tree-ring record (Grissino-Mayer et al., 1997; Van West and Grissino-Mayer, 2005).

1200–1000 cal yr BP

Between ~1200 and 1000 cal yr BP, a muddy cumulic soil (stratum IIIc) formed at Cienega Amarilla in areas surrounding the spring mound. The absence of riparian or aquatic indicators in the pollen and macrobotanical records suggests continued drying. Although GWD was reduced compared to the 2300–1500 cal yr BP interval, continued tufa deposition at the spring mound suggests that discharge was nonetheless higher than before 2300 cal yr BP. The resumption of floodplain aggradation during the 1200–1000 cal yr BP period at Cottonwood Canyon implies increased runoff and sediment yield from hillslopes perhaps related to reduced vegetation cover caused by drought or fire.

1000 cal yr BP to present

Alluvium younger than ~1000 cal yr BP at Cienega Amarilla is dominated by sandy floodplain facies (strata IV–VI) that indicate a shift from a GWD-dominated floodplain system to one dominated by surface runoff. A distinct, ^{14}C-dated burned layer with C_4 grass macrofossils implies summer and winter drought ~900–800 cal yr BP. Arroyo cutting between ~1000 and 650 cal yr BP at Cottonwood Canyon likely resulted in downstream deposition of alluvium (stratum IV) in the Cienega Amarilla area. A brief soil-forming period lasting less than a century was followed by another period of valley aggradation (stratum V) from ~650 to 100 cal yr BP. Historical-period arroyo cutting resulted in some areas being mantled by recent distributary fan alluvium (stratum VI).

Climatic drivers of Cienega Amarilla GWD

The isotopic composition of Cienega Amarilla springwater more closely resembles that of cool-season precipitation (Table 3, Fig. 10), suggesting that GWD is derived mostly from October–April precipitation. Although modern cool-season precipitation totals in the Cienega Amarilla area are generally smaller than warm-season totals, winter and early spring moisture is hydrologically more important than summer rains. Winter and early spring storms are generally more widespread, lower intensity, longer duration, and coincide with cooler temperatures and dormant vegetation; these conditions result in decreased surface runoff and less evaporative and evapotranspirative loss (Bryson and Hare, 1974; Trewartha, 1981; Barry and Chorley, 1998). Thus, groundwater recharge (and discharge) in the southwestern United States is derived primarily from cool-season precipitation because more winter moisture infiltrates into the ground (Eastoe et al., 2004), and this generalization appears valid at Cienega Amarilla.

Comparison to other southwestern US records

Other well-dated, climatically sensitive, late Holocene paleoenvironmental records in the larger southwestern US region corroborate both the distinct period of increased effective moisture ~2300–1500 cal yr BP and the subsequent drying trend documented at Cienega Amarilla (Supplementary Figure 1). The southwestern US regional shift to drought conditions ~1600 cal yr BP appears to be an expression of global-scale changes including a major climate and vegetation shift that later culminated during the ~1050–650 cal yr BP Medieval Climate Anomaly (MCA) (Viau et al., 2002; Mayewski et al., 2004), including especially severe drought ~800 cal yr BP (Cook et al., 2004, 2014; Woodhouse et al., 2010).

Moisture-sensitive tree-ring records in the Southwest largely reflect cool-season moisture because most of the annual ring forms as early wood during the spring and early summer (Fritts, 2001). The smoothed tree-ring record at El Malpais, located ~100 km northeast of Cienega Amarilla, suggests generally moister-than-average conditions during the ~2100–1700 cal yr BP interval (Grissino-Mayer, 1996). This record's most severe long-term drought is a 263-yr-long period from ~1700 to 1450 cal yr BP, with especially arid conditions after ~1600 cal yr BP (Grissino-Mayer, 1996; Grissino-Mayer et al., 1997). The San Francisco Peaks tree-ring record in north-central Arizona indicates above average temperatures from 1600 to 1250 cal yr BP (Salzer, 2000; Van West and Grissino-Mayer, 2005) that culminated in a pronounced, ~1300–1100 cal yr BP warming trend evident in tree-ring records throughout western North America (Trouet et al., 2013).

Oxygen isotope data suggest that southwestern cave records are proxies generally more biased toward reflecting winter rather than summer precipitation amounts, especially during the past several thousand years (Truebe et al., 2010). Although speleothem annual band thickness and δ^{18}O records in the Guadalupe Mountains of southeastern New Mexico suggest greatest late Holocene effective moisture there between ~2800 and 2600 cal yr BP, a secondary peak was evident ~2000 cal yr BP, and thinner bands or aragonite

https://doi.org/10.1017/qua.2016.14 Published online by Cambridge University Press

layers from ~1700 to 1300 cal yr BP imply drier conditions (Polyak and Asmeron, 2001; Asmerom et al., 2007).

The $\delta^{13}C$ composition of ^{14}C-dated sediment at Abo Arroyo in central New Mexico suggests a late Holocene interval of cooler temperatures and wetter winters that was most pronounced from ~2400 to 1400 cal yr BP and then ended abruptly (Hall and Penner, 2013). Aquatic plant macrofossils in the ~10,000 yr record at Stoneman Lake in central Arizona were most abundant from ~2000 to 1600 cal yr BP, suggesting high lake levels and increased effective moisture during this period (Hasbargen, 1994). Similarly, mollusks at the La Playa archaeological site in northern Sonora, Mexico, imply peak GWD from ~2300 to 1600 cal yr BP (Copeland et al., 2012). In southern Nevada, the resumption of black mat formation beginning ~2300 cal yr BP after a ~4500 yr hiatus implies enhanced GWD associated with increased winter precipitation (Quade et al., 1998; Winograd et al., 1998). A high-resolution pollen record from Lower Pahranagat Lake in southern Nevada suggests a ~2100–2000 cal yr BP climate event characterized by dramatic increases in pine, juniper, and sagebrush pollen interpreted to indicate unusually wet winters (Wigand and Rhode, 2002).

In summary, a variety of paleoenvironmental proxies from across the Southwest region suggest a period of unusually wet winters from ~2300 to 1500 cal yr BP followed by a distinct drying trend leading up to the MCA. Therefore, the distinct, latest Holocene period of enhanced cool-season precipitation evident at Cienega Amarilla appears to be part of a broader pattern driven by large-scale meteorological processes.

Historical cool-season precipitation variability

Climate divisions are areas of general modern climate homogeneity. Statistical analysis of historical climate division data from 1905 to 2005 indicates significantly ($P < 0.05$) increased (decreased) winter precipitation during El Niño (La Niña) years across the southern United States, with very high correlation ($P < 0.0001$) for the climate division containing Cienega Amarilla (Kurtzman and Scanlon, 2007). Between 1895 and 1996 the climate division containing Cienega Amarilla received 67% more December–March precipitation during El Niño years than during non–El Niño years (Lenart, 2006). At the nearest weather station with a relatively complete precipitation record (Springerville, AZ), El Niño winters (December–March) from 1950–2004 were on average 18% wetter than normal, and La Niña winters were 22% drier (Western Regional Climate Center, 2016) (Fig. 12a).

Kurtzman and Scanlon (2007) found that PDO phase has a significant ($P < 0.1$) effect on winter precipitation amount only in the south-central United States, including the climate division containing Cienega Amarilla, where the effect is relatively pronounced (with a P value in the 0.0011–0.01 range). The strengthening of El Niño (La Niña) positive (negative) anomalies during a PDO warm (cold) phase and reducing this effect during a PDO cold (warm) phase is known as the El Niño (La Niña) Decadal Modulation (Kurtzman and Scanlon, 2007). The Southwest, including Cienega Amarilla, is subject more to the effects of the El Niño Decadal Modulation than to the La Niña Decadal Modulation (Brown and Comrie, 2004; Kurtzman and Scanlon, 2007). We evaluated the effect of PDO on winter precipitation at Cienega Amarilla by pooling Springerville 1950–2004 monthly precipitation data by season, splitting the data into six ENSO and PDO phase categories, and calculating precipitation deviations by subtracting the long-term mean from the category-mean (Fig. 12b). Mean seasonal anomalies at Cienega Amarilla show (1) a strong El Niño Decadal Modulation effect (28% above normal winter precipitation during positive PDO and 4% below normal during negative PDO); (2) a weak La Niña Decadal Modulation effect (24% below normal during negative PDO and 19% below normal during positive PDO); and (3) near-normal cool-season precipitation for ENSO neutral years during both cold and warm PDO phases.

Possible century-scale paleoclimatic teleconnections

Cienega Amarilla likely experienced prehistoric periods with significantly greater cool-season precipitation than represented in the historical climate record. The study area lies immediately east of areas that presently receive more winter precipitation and have a more pronounced bimodal precipitation pattern (Sheppard et al., 2002: fig. 3). The boundary between the two precipitation patterns is determined by the relative strengths of the air masses that bring winter and summer moisture, and its location has shifted over time (Dean, 1988). McGregor and Gagan (2004) argue that equatorial western and central Pacific coral $\delta^{18}O$ records indicate that more severe and longer El Niño events occurred in the past than are evident in the modern instrumental record. Based on terrestrial and marine proxies from sites along the northeastern Pacific margins, Barron and Anderson (2011) concluded that many western North America spatial climate patterns and shifts during the Holocene are related to changes in ENSO and PDO phases. They concluded that the establishment of modern climate conditions between 4200 and 3000 cal yr BP at the beginning of the late Holocene involved a shift to more variable, El Niño–like, and warm PDO-like conditions in the Pacific Ocean that resulted in an intensified or eastwardly shifted wintertime Aleutian Low and a weaker or more southwardly displaced North Pacific High.

Climatic teleconnections between the subtropical and North Pacific and spatial precipitation patterns in western North America during the Holocene are better understood at annual to decadal scales than at century to millennial scales (Barron and Anderson, 2011). At Cienega Amarilla, an abrupt shift to a GWD-dominated system ~2300 cal yr BP and transition back to a runoff-dominated system ~1000 cal yr BP imply significant changes in winter precipitation. Assuming that annual- and decadal-scale atmospheric processes can be extrapolated to longer time scales because of

https://doi.org/10.1017/qua.2016.14 Published online by Cambridge University Press

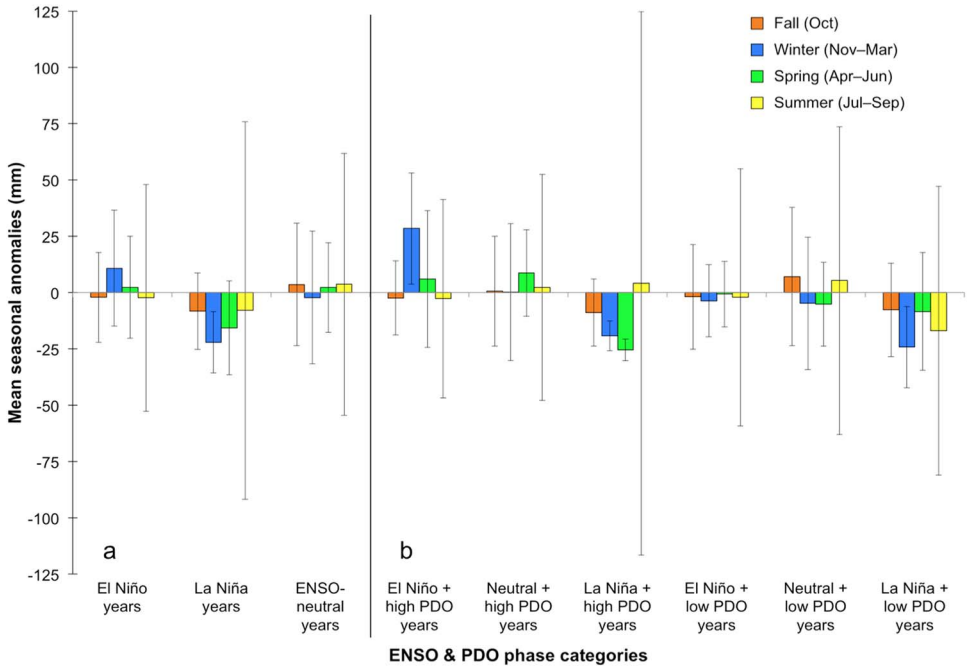

Figure 12. (color online) Seasonal precipitation anomalies of (a) ENSO phases and (b) ENSO and PDO phase combinations based on Springerville, Arizona, historical climate data from 1950 to 2004. Monthly data were pooled by season, and two PDO phases are represented (low from 1950 to 1977 and high from 1978 to 2004) per Kurtzman and Scanlon (2007). ENSO and PDO phase of each year as identified by Guan et al. (2005). Standard deviation (1σ) bars show temporal variability. ENSO, El Niño–Southern Oscillation; PDO, Pacific Decadal Oscillation.

the coherency of atmospheric dynamics, these changes suggest an interval of unusually strong and frequent El Niños and persistently warm PDO conditions in the Pacific from ~2300 to 1500 cal yr BP that resulted in unusually wet winters in the southwestern United States.

El Niño proxies

Modeling studies and proxy evidence from the eastern equatorial Pacific indicate peak late Holocene ENSO activity between ~2800 and 1600 cal yr BP (Fig. 11) that implies a more positive/warm PDO phase in the North Pacific (Barron and Anderson, 2011). A proxy record of the strength of NAM circulation provided by the relative abundance of *Globigerinoides sacculifer* from Gulf of Mexico seafloor sediment cores suggests that this period of stronger and more frequent El Niño events was preceded by substantial weakening of monsoonal circulation from ~3000 to 2800 cal yr BP (Fig. 11) (Poore et al., 2005).

Using El Junco Crater Lake sediment core grain-size data from the Galápagos Islands in the core ENSO area, Conroy et al. (2008) identified an interval of peak Holocene El Niño frequency between 2000 ± 100 and 1500 ± 70 cal yr BP that is roughly coincident with the Cienega Amarilla pluvial (Fig. 11). Annually resolved, equatorial coral $\delta^{18}O$ records from the northern and central equatorial Pacific similarly suggest anomalously extreme and prolonged El Niño events between 2500 and 1700 cal yr BP, including a 4 yr event with almost twice the amplitude of the 1997–1998 event and a 7 yr event that is longer than any known Holocene or modern event (McGregor and Gagan, 2004) (Fig. 11). The Cienega Amarilla ~1500–1000 cal yr BP drying trend is similarly consistent with Conroy et al.'s (2008) Galápagos record, which indicates El Niño frequency decreased precipitously after ~1600 cal yr BP and remained especially low until ~1300 cal yr BP, implying diminished winter precipitation during this period in the southwestern United States.

Archaeological implications

Springs are sacred places of power to Southwest indigenous people (Rea, 2008), and Cienega Amarilla was undoubtedly a focus of prehistoric human activity during the late Holocene. The springs not only provided a reliable freshwater source, but also attracted game and waterfowl and offered unique riparian and paludal plant resources including cattail. Cattail pollen has a high caloric return (Simms, 1987) and remains important in contemporary Puebloan religious practices (Parsons, 1939). On a regional scale, Pueblo I (1200–1050 cal yr BP) villages were often established near marshes, and later Puebloans inhabiting places lacking natural wetlands often created artificial marshes by constructing reservoirs (Anderson and Potter, 2015).

Several large Pueblo II (1050–800 cal yr BP) and Pueblo III (800–650 cal yr BP) period archaeological surface sites are recorded within several kilometers of the Cienega Amarilla spring mound. Buried Basketmaker II (2450–1450 cal yr BP), Pueblo I (1200–1050 cal yr BP), and Protohistoric (500–350 cal yr BP) period sites discovered during this study

https://doi.org/10.1017/qua.2016.14 Published online by Cambridge University Press

at Cottonwood Canyon are intriguing because sites dating to these cultural periods are poorly represented in the surrounding area (Huber, 2005). Directly dated maize macrofossils from thermal features at these sites suggest maize agriculture was practiced ~2150 and 1100 cal yr BP in the Cienega Amarilla area (Table 1).

The 2300–1500 cal yr BP interval of substantially increased effective moisture indicated by the Cienega Amarilla stratigraphic record and corroborated by numerous other paleoenvironmental proxies probably resulted in improved conditions for maize agriculture over much of the Southwest region. Increased areas with shallow groundwater would have encouraged water-table farming, a strategy that Mabry (2005) argued was a highly optimal agricultural niche in terms of risk, labor, yield, and efficiency. Although areas suitable for groundwater farming were probably not extensive, increased cool-season precipitation likely resulted in widespread, consistently favorable conditions for dryland and floodwater farming. Residual winter and early spring soil moisture can extend the maize growing season by making seed germination possible well before the onset of the summer monsoon, thereby increasing the odds of a successful crop, especially at low and middle elevations.

The ~2300–1500 cal yr BP period of inferred peak cool-season precipitation at Cienega Amarilla during the late Holocene coincides with significant cultural change in the American Southwest. During this interval, prehistoric human populations grew and became more sedentary and dependent on agriculture; these changes are evident at Basketmaker II sites on the southern Colorado Plateau and Cienega phase sites in central and southeastern Arizona (Cordell and McBrinn, 2012). This pattern extended south into northern Sonora, Mexico, and is typified by the La Playa site, where peak human occupation from 2300 to 1500 cal yr BP was followed by a sharp decline (Copeland et al., 2012). It seems reasonable to speculate that enhanced cool-season precipitation in the Southwest region resulting from more frequent and/or stronger El Niño events and persistently high PDO conditions at this time were a catalyst for these cultural changes.

CONCLUSIONS

Cool-season precipitation at Cienega Amarilla exceeded a local hydrologic threshold ~2300 cal yr BP, causing a shift from runoff-dominated to groundwater discharge–dominated floodplain processes. Markedly increased GWD indicated by rapid growth of a tufa spring mound and development of a surrounding marsh during the ~2300–1500 cal yr BP interval was followed by a sudden and pronounced decline during the 1500–1000 cal yr BP interval. The ~2300–1500 cal yr BP period of enhanced GWD at Cienega Amarilla may be linked to more frequent or stronger El Niños and persistently warm (positive) PDO conditions that surpass those evident in the modern instrumental record. Recognition of this interval contributes to our understanding of teleconnections between Pacific climate patterns and spatial precipitation patterns in western North America at centennial time scales. Modern El Niño events coinciding with warm PDOs usually result in wetter than normal winters in the south-central United States (New Mexico through Louisiana) (Kurtzman and Scanlon, 2007), and it is plausible that this spatial precipitation pattern extends back several millennia. The ~2300–1500 cal yr BP interval of increased cool-season moisture coincides with significant cultural changes during the Basketmaker II period on the southern Colorado Plateau and the Cienega phase in central and southeastern Arizona and northern Sonora. These changes—which include increased sedentism, dependence on maize agriculture, and population growth—may have been fostered by increased cool-season precipitation.

ACKNOWLEDGMENTS

This research was funded by the National Science Foundation (NSF) (Doctoral Dissertation Improvement Grant #1041950 and IGERT Fellowship in Archaeological Science); the Geological Society of America (Graduate Student Research Grant and Claude C. Albritton Jr. Scholarship Award); the Philanthropic Educational Organization (Scholar Award); the Colorado Scientific Society (William G. Pierce Research Grant); the Charles Redd Center for Western Studies (Graduate Student Summer Fieldwork Award); the NSF-Arizona Accelerated Mass Spectrometry Laboratory; the Argonaut Archaeological Research Fund; and the University of Arizona Department of Geosciences (Dr. H. Wesley Peirce, Bert Butler, and Keith L. Katzer scholarships). Brenda Wilkinson and David Simons (Bureau of Land Management) and David Eck (New Mexico State Land Office) provided permits (BLM permit 273-8152-11; NMSLO ROE-1712 and CPRC Project-Specific permit #SE-300). We thank Susanne and the late Clifford Thorn and Mark Hubbell (landowners); David Dettman (isotope analysis); John Douglass and Shane Miller (fieldwork help); Barbara Mills, Dean Wilson, Matt Peeples, and Patricia Gilman (ceramic identification); and Zackry Guido and Jan Null (climate information). This research benefitted from discussions with Vance Haynes, Stephen Hall, and Jordon Bright. An early version of the manuscript benefitted from input by Jay Quade, Vance Holliday, and Barbara Mills. Lastly, we appreciate the thorough and constructive peer reviews provided by Jeff Pigati and two anonymous reviewers.

Supplementary material

To view supplementary material for this article, please visit https://doi.org/10.1017/qua.2016.14

REFERENCES

Adams, D.K., Comrie, A.C., 1997. The North American monsoon. *Bulletin of the American Meteorological Society* 78, 2197–2213.

Akers, J.P., 1964. Geology and ground water in the central part of Apache County, Arizona. Geological Survey Water-Supply Paper 1771. US Government Printing Office, Washington, D.C.

Anderson, K.C., Potter, J.M., 2015. Chronostratigraphic and paleoenvironmental evidence for marsh habitats during the Early Pueblo I (AD 700–900) occupation of Ridges Basin, southwest Colorado, USA. *Geoarchaeology: An International Journal* 30, 110–119.

Andrade, E.R., Jr., Sellers, W.D., 1988. El Niño and its effect on precipitation in Arizona and western New Mexico. *Journal of Climatology* 8, 403–410.

Asmerom, Y., Polyak, V., Burns, S., Rassmussen, J., 2007. Solar forcing of Holocene climate: new insights from a speleothem record, southwestern United States. *Geology* 35(1), 1–4. http://dx.doi.org/10.1130/G22865A.1.

Barron, J.A., Anderson, L., 2011. Enhanced late Holocene ENSO/PDO expression along the margins of the eastern North Pacific. *Quaternary International* 235, 3–12.

Barry, R.G., Chorley, R.J., 1998. *Atmosphere, Weather and Climate*. 7th ed. Routledge, London.

Basabilvazo, G.T., 1997. *Ground-Water Resources of Catron County, New Mexico*. US Department of the Interior, US Geological Survey, Albuquerque, NM.

Basch, P., 1963. A review of the recent freshwater Limpet snails of North America (Mollusca: Pulmonata). *Bulletin of the Museum of Comparative Zoology at Harvard College* 129(8), 399–461.

Brown, D.P., Comrie, A.C., 2004. A winter precipitation "dipole" in the western United States associated with multidecadal ENSO variability. *Geophysical Research Letters* 31, L09203. http://dx.doi.org/10.1029/2003GL018726.

Bryson, R.A., Hare, F.K., 1974. The climates of North America. In: Bryson, R.A., Hare, F.K. (Eds.), *Climates of North America*. Elsevier, New York, pp. 1–47.

Chamberlain, R.M., Cather, S.M., Anderson, O.J., Jones, G.E., 1994. Reconnaissance Geologic Map of the Quemado 30 x 60 Minute Quadrangle, Catron County, New Mexico. Open-File Report 406. New Mexico Bureau of Mines and Mineral Resources, Socorro, NM.

Conroy, J.L., Overpeck, J.T., Cole, J.E., Shanahan, T.M., Steinitz-Kannan, M., 2008. Holocene changes in eastern tropical Pacific climate inferred from a Galápagos lake sediment record. *Quaternary Science Reviews* 27, 1166–1180. http://dx.doi.org/10.1016/j.quascirev.2008.02.015.

Cook, B.I., Smerdon, J.E., Seager, R., Cook, E.R., 2014. Pan-continental droughts in North America over the last millennium. *Journal of Climate* 27, 383–397.

Cook, E.R., Woodhouse, C.A., Eakin, C.M., Meko, D.M., Stahle, D.W., 2004. Long-term aridity changes in the western United States. *Science* 306, 1015–1018. http://dx.doi.org/10.1126/science.1102586.

Copeland, A., Quade, J., Watson, J.T., McLaurin, B.T., Villalpando, E., 2012. Stratigraphy and geochronology of La Playa archaeological site, Sonora, Mexico. *Journal of Archaeological Science* 39, 2934–2944. http://dx.doi.org/10.1016/j.jas.2012.04.034.

Cordell, L.S., McBrinn, M.E., 2012. *Archaeology of the Southwest*. 3rd ed. Left Coast Press, Walnut Creek, CA.

Dean, J.S., 1988. Dendrochronology and paleoenvironmental reconstruction on the Colorado Plateaus. In: Gumerman, G.J. (Ed.), *The Anasazi in a Changing Environment*. Cambridge University Press, Cambridge, pp. 119–167.

Eastoe, C.J., Gu, A., Long, A., 2004. The origins, ages and flow paths of groundwater in Tucson basin: results of a study of multiple isotope systems. In: Hogan, J.F., Phillips, F.M., Scanlon, B.R. (Eds.), *Groundwater Recharge in a Desert Environment—The Southwestern United States. Water Science and Application 9*. American Geophysical Union, Washington, DC, pp. 217–234.

Embid, E.H., 2009. U-Series Dating, Geochemistry, and Geomorphic Studies of Travertines and Springs of the Springerville Area, East-Central Arizona, and Tectonic Implications. Master's thesis, University of New Mexico, Albuquerque.

Evanoff, E., 1987. Appendix 4: fossil nonmarine snails from the Horner Site. In: Frison, G.C., Todd, L.C. (Eds.), *The Horner Site: The Type Site of the Cody Complex*. Academic Press, Orlando, FL, pp. 443–450.

Fritts, H.C., 2001. *Tree Rings and Climate*. Blackburn Press, Caldwell, NJ.

Forester, R.M., 1988. Nonmarine calcareous microfossil sample preparation and data acquisition procedures. *US Geological Survey Technical Procedure HP-78*, R1, 1–9.

Forester, R.M., 1991. Ostracode assemblages from springs in the western United States: implications for paleohydrology. *Memoirs of the Entomological Society of Canada* 155, 181–201.

Forester, R.M., Smith, A.J., 1994. Late glacial climate estimates for southern Nevada: the ostracode fossil record. Proceedings of the 5th Annual International High-Level Radioactive Waste Management Conference and Exposition, Las Vegas, Nevada, May 22–26, 1994. *American Nuclear Society, LaGrange, IL*, vol. 4, pp. 2553–2561.

Grissino-Mayer, H.D., 1996. A 2129-year reconstruction of precipitation for northwestern New Mexico, USA. In: Dean, J.S., Meko, D.M., Swetnam, T.W. (Eds.), Tree Rings, Environment, and Humanity: Proceedings of the International Conference, Tucson, Arizona, 17–21 May 1994. Radiocarbon, Department of Geosciences, University of Arizona, Tucson, pp. 191–204.

Grissino-Mayer, H.D., Swetnam, T.W., Adams, R.K., 1997. The rare old-aged conifers of El Malpais: their role in understanding climate change in the American Southwest. *New Mexico Bureau of Mines and Mineral Resources Bulletin* 156, 155–161.

Guan, H., Vivoni, E.R., Wilson, J.L., 2005. Effects of atmospheric teleconnections on seasonal precipitation in mountainous regions of the southwestern U.S.: a case study in northern New Mexico. *Geophysical Research Letters* 32, L23701. http://dx.doi.org/10.1029/2005GL023759.

Hall, S.A., Penner, W.L., 2013. Stable carbon isotopes, C3–C4 vegetation, and 12,800 years of climate change in central New Mexico, USA. *Palaeogeography, Palaeoclimatology, Palaeoecology* 369, 272–281. http://dx.doi.org/10.1016/j.palaeo.2012.10.034.

Hall, S.A., Penner, W., Ellis, M., 2009. Arroyo cutting and vegetation change in Abo Canyon, New Mexico: evidence from repeat photography along the Santa Fe Railway. In: Lueth, V.W., Lucas, S.G., Chamberlin, R.M. (Eds.), Geology of the Chupadera Mesa: New Mexico Geological Society 60th Annual Field Conference, October 7–10, 2009. New Mexico Geological Society, Socorro, NM, pp. 429–438.

Hasbargen, J., 1994. A Holocene paleoclimatic and environmental record from Stoneman Lake, Arizona. *Quaternary Research* 42, 188–196.

Haynes, C.V., Jr., 2008. Quaternary cauldron springs as paleoecological archives. In: Stevens, L.E., Meretsky, V.J. (Eds.), *Aridland Springs in North America: Ecology and Conservation*. University of Arizona Press, Tucson, pp. 76–97.

Hershler, R., Sada, D.W., 2002. Biogeography of Great Basin aquatic snails of the genus *Pyrgulopsis*. In: Hershler, R., Madsen, D.B., Currey, D.R. (Eds.), *Great Basin Aquatic Systems History. Smithsonian Contributions to the Earth Sciences 33*. Smithsonian Institution, Washington, DC, pp. 255–276.

Huber, E.K., 2005. Settlement patterns in the Fence Lake Project area. In: Huber, E.K., Van West, C.R. (Eds.), *Fence Lake Project: Archaeological Data Recovery in the New Mexico Transportation Corridor and First Five-Year Permit Area, Fence Lake Coal Mine Project, Catron County, New Mexico. Vol. 4, Synthetic*

Studies and Summary. Technical Series 84. Statistical Research Inc., Tucson, AZ, pp. 39.1–39.53.

International Atomic Energy Agency and World Meteorological Organization. 2015. Global Network of Isotopes in Precipitation (GNIP) Database (accessed October 8, 2015). http://www-naweb.iaea.org/napc/ih/IHS_resources_gnip.html.

Janitzky, P., 1986. Organic carbon (Walkley-Black method). In: Singer, M.J., Janitsky, P. (Eds.), *Field and Laboratory Procedures Used in a Soil Chronosequence Study. US Geological Survey Bulletin 1648*. US Government Printing Office, Washington, DC, pp. 30–33.

Karanovic, I., 2012. *Recent Freshwater Ostracods of the World: Crustacea, Ostracoda, Podocopida*. Springer, Heidelberg, Germany.

Kiladis, G.N., Diaz, H.F., 1989. Global climate anomalies associated with extremes of the Southern Oscillation. *Journal of Climate* 2, 1069–1090.

Kreamer, D.K., Springer, A.E., 2008. The hydrology of desert springs in North America. In: L.E. Stevens, Meretsky, V.J. (Eds.), *Aridland Springs in North America: Ecology and Conservation*. University of Arizona Press, Tucson, pp. 35–48.

Kurtzman, D., Scanlon, B.R., 2007. El Niño–Southern Oscillation and Pacific Decadal Oscillation impacts on precipitation in the southern and central United States: evaluation of spatial distribution and predictions. *Water Resources Research* 43, W10427. http://dx.doi.org/10.1029/2007WR005863.

Lebron, I., Herrero, J., Robinson, D.A., 2009. Determination of gypsum content in dryland soils exploiting the gypsum–bassanite phase change. *Soil Science Society of America Journal* 73, 403–411. http://dx.doi.org/10.2136/sssaj2008.0001.

Lenart, M., 2006. El Niño: a wild card for climate change impacts. Southwest Climate Outlook (January 24), 2–4. http://www.climas.arizona.edu/sites/default/files/janpacket2006_1.pdf.

Mabry, J., 2005. Diversity in early southwestern farming systems and optimization models of transitions to agriculture. In: Diehl, M.W., (Ed.), Subsistence and Resource Use Strategies of Early Agricultural Communities in Southern Arizona. Anthropological Papers No. 34. Center for Desert Archaeology, Tucson, AZ, pp. 113–152.

Machette, M., 1986. Calcium and magnesium carbonates. In: Singer, M.J., Janitsky, P. (Eds.), *Field and Laboratory Procedures Used in a Soil Chronosequence Study. US Geological Survey Bulletin 1648*. US Government Printing Office, Washington, DC, pp. 30–33.

Magnani, M.B., Miller, K.C., Levander, A., Karlstrom, K., 2004. The Yavapai-Mazatzal boundary: a long-lived tectonic element in the lithosphere of southwestern North America. *Geological Society of America Bulletin* 116, 1137–1142.

Mayewski, P.A., Rohling, E.E., Stager, J.C., Karlén, W., Maasch, K.A., Meeker, L.D., Meyerson, E.A., *et al.*, 2004. Holocene climate variability. *Quaternary Research* 62, 243–255. http://dx.doi.org/10.1016/j.yqres.2004.07.001.

Mayo, E.B., 1958. Lineament tectonics and some ore districts of the Southwest. *Mining Engineering* 10, 1169–1175.

McGregor, H.V., Gagan, M.K., 2004. Western Pacific coral $\delta^{18}O$ records of anomalous Holocene variability in the El Niño–Southern Oscillation. *Geophysical Research Letters* 31, L11204. http://dx.doi.org/10.1029/2004GL019972.

Moore, J., Adams, M., Allis, R., Lutz, S., Rauzi, S., 2005. Mineralogical and geochemical consequences of the long-term presence of CO_2 in natural reservoirs: an example from the Springerville–St. Johns Field, Arizona, and New Mexico, U.S.A. *Chemical Geology* 217, 365–385.

New Mexico Bureau of Geology and Mineral Resources. 2003. *Geologic Map of New Mexico, Scale 1:500,000*. New Mexico Bureau of Geology and Mineral Resources, Socorro, NM.

O'Brien, B.R., 1956. Geology of Cienega Amarilla Area, Catron County, New Mexico and Apache County, Arizona. Master's thesis, University of Texas, Austin.

Ogle, D.G., St. John, L., Tilley, D., 2012. *Plant Guide for Fourwing Saltbush (Atriplex canescens)*. US Department of Agriculture, Natural Resources Conservation Service, Plant Materials Center, Aberdeen, ID.

Onken, J., 2015. Late Quaternary Climatic Geomorphology, Volcanism, and Geoarchaeology of Carrizo Wash, Little Colorado River Headwaters, USA. PhD dissertation, University of Arizona, Tucson.

Palacios-Fest, M.R., 1994. Nonmarine ostracode shell chemistry from Hohokam irrigation canals in central Arizona: a paleohydrochemical tool for the interpretation of prehistoric human occupation in the North American Southwest. *Geoarchaeology* 9(1), 1–29.

Palacios-Fest, M.R., 2010. Late Holocene paleoenvironmental history of the upper west Amarillo Creek valley at archaeological site 41PT185/C, Texas, USA. *Boletín de la Sociedad Geológica Mexicana* 62, 399–436.

Parsons, E.C., 1939. *Pueblo Indian Religion*. University of Chicago Press, Chicago.

Pigati, J.S., Rech, J.A., Nekola, J.C., 2010. Radiocarbon dating of small terrestrial gastropod shells in North America. *Quaternary Geochronology* 5, 519–532. http://dx.doi.org/10.1016/j.quageo.2010.01.001.

Pigati, J.S., Rech, J.A., Quade, J., Bright, J., 2014. Desert wetlands in the geologic record. *Earth-Science Reviews* 132, 67–81. http://dx.doi.org/10.1016/j.earscirev.2014.02.001.

Pigati, J.S., Quade, J., Shahanan, T.M., Haynes, C.V., Jr., 2004. Radiocarbon dating of minute gastropods and new constraints on the timing of late Quaternary spring discharge deposits in southern Arizona, USA. *Palaeogeography, Palaeoclimatology, Palaeoecology* 204, 33–45. http://dx.doi.org/10.1016/S0031-0182(03)00710-7.

Polyak, V.J., Asmerom, Y., 2001. Late Holocene climate and cultural changes in the southwestern United States. *Science* 294, 148–151. http://dx.doi.org/10.1126/science.1062771.

Poore, R.Z., Pavich, M.J., Grissino-Mayer, H.D., 2005. Record of the North American southwest monsoon from Gulf of Mexico sediment cores. *Geology* 33(3), 209–212. http://dx.doi.org/10.1130/G21040.1.

Quade, J., Forester, R.M., Pratt, W.L., Carter, C., 1998. Black mats, spring-fed streams, and late-glacial-age recharge in the southern Great Basin. *Quaternary Research* 49, 129–148. http://dx.doi.org/10.1006/qres.1997.1959.

Quade, J., Rech, J.A., Betancourt, J.L., Latorre, C., Quade, B., Rylander, K.A., Fisher, T., 2008. Paleowetlands and regional climate change in the central Atacama Desert, northern Chile. *Quaternary Research* 69, 343–360. http://dx.doi.org/10.1016/j.yqres.2008.01.003.

Ramsey, C.B., 2009. Bayesian analysis of radiocarbon dates. *Radiocarbon* 51, 337–360.

Rea, A.M., 2008. Historic and prehistoric ethnobiology of desert springs. In: Stevens, L.E., Meretsky, V.J. (Eds.), *Aridland Springs in North America: Ecology and Conservation*. University of Arizona Press, Tucson, pp. 268–278.

Reimer, P.J., Bard, E., Bayliss, A., Beck, J.W., Blackwell, P.G., Ramsey, C.B., Buck, C.E., 2013. IntCal13 and Marine13

radiocarbon age calibration curves 0–50,000 years cal BP. *Radiocarbon* 55(4), 1869–1887.

Salzer, M.W., 2000. Dendroclimatology in the San Francisco Peaks Region of Northern Arizona, USA. PhD dissertation, University of Arizona, Tucson.

Schumacher, B.A., 2002. *Methods for the determination of total organic carbon (TOC) in soils and sediments. NCEA-C- 1282, EMASC-001*. US Environmental Protection Agency, Washington, DC.

Sheppard, P.R., Comrie, A.C., Packin, G.D., Angersbach, K., Hughes, M.K., 2002. The climate of the US Southwest. *Climate Research* 21, 219–238.

Simms, S.R., 1987. Behavioral Ecology and Hunter-Gatherer Foraging: An Example from the Great Basin. British Archaeological Reports (BAR) International Series 381. BAR, Oxford.

Smith, S.J., 1998. Processing pollen samples from archaeological sites in the southwestern United States: an example of differential recovery from two heavy liquid separation procedures. In: Bryant, V.M., Wrenn, J.H. (Eds.), *New Developments in Palynomorph Sampling, Extraction, and Analysis. Contributions Series No. 33*. American Association of Stratigraphic Palynologists Foundation, Houston, TX, pp. 29–34.

Smith, W., 1986. *The Effects of Eastern North Pacific Tropical Cyclones on the Southwestern United States. NOAA Technical Memorandum NWS WR-197*. US Department of Commerce, National Oceanic and Atmospheric Administration, National Weather Service, Western Region, Salt Lake City, UT.

Trenberth, K.E., Branstator, G.W., Karoly, D., Kumar, A., Lau, N.C., Ropelewski, C., 1998. Progress during TOGA in understanding and modeling global teleconnections associated with tropical sea surface temperatures. *Journal of Geophysical Research* 103, 14291–14324.

Trewartha, G.T., 1981. *The Earth's Problem Climates*. University of Wisconsin Press, Madison.

Trouet, V., Diaz, H.F., Wahl, E.R., Viau, A.E., Graham, R., Graham, N., Cook, E.R., 2013. A 1500-year reconstruction of annual mean temperature for temperate North America on decadal-to-multidecadal time scales. *Environmental Research Letters* 8, 024008. http://dx.doi.org/10.1088/1748-9326/8/2/024008.

Truebe, S.A., Ault, T.R., Cole, J.E., 2010. A forward model of cave dripwater $\delta^{18}O$ and application to speleothem records. IoP Conference Series: Earth and Environmental Science 9, 1–8.

Van West, C.R., Grissino-Mayer, H.D., 2005. Dendroclimatic reconstruction. In: Huber, E.K., Van West, C.R. (Eds.), *Fence Lake Project: Archaeological Data Recovery in the New Mexico Transportation Corridor and First Five-Year Permit Area, Fence Lake Coal Mine Project, Catron County, New Mexico. Vol. 3, Environmental Studies. Technical Series 84*. Statistical Research Inc., Tucson, AZ, pp. 33.1–33.129.

Viau, A.E., Gajewski, K., Fines, P., Atkinson, D.E., Sawada, M.C., 2002. Widespread evidence of 1500 yr climate variability in North America during the past 14,000 yr. *Geology* 30(5), 455–458.

Wagner, J.D.M., Cole, J.E., Beck, J.W., Patchett, P.J., Henderson, G.M., Barnett, H.R., 2010. Moisture variability in the southwestern United States linked to abrupt glacial climate change. *Nature Geoscience* 3, 110–113. http://dx.doi.org/10.1038/ngeo707.

Walkley, A., Black, I.A., 1934. An examination of the Degtjareff method for determining organic carbon in soils: effect of variations in digestion conditions and of inorganic soil constituents. *Soil Science* 63, 251–263.

Wang, C., Deser, C., Yu, J.Y., DiNezio, P., Clement, A., 2016. El Niño and Southern Oscillation (ENSO): a review. In: Glynn, P., Manzello, D., Enochs, I. (Eds.), *Coral Reefs of the Eastern Tropical Pacific: Persistence and Loss in a Dynamic Environment. Coral Reefs of the World 8*. Springer, Berlin, pp. 85–106.

Waters, M.R., Haynes, C.V., 2001. Late Quaternary arroyo formation and climate change in the American Southwest. *Geology* 29, 399–402.

Western Regional Climate Center, 2016. Historical Data: Cooperative Climatological Data Summaries, Arizona (accessed June 15, 2016). http://www.wrcc.dri.edu/summary/Climsmaz.html.

Wigand, P.E., Rhode, D., 2002. Great Basin vegetation history and aquatic systems: the last 150,000 years. In: Hershler, R.S., Madsen, D.B., Currey, D.R. (Eds.), *Great Basin Aquatic Systems History. Smithsonian Contributions to Earth Sciences 33*. Smithsonian Institution Press, Washington, DC, pp. 309–367.

Winograd, I.J., Riggs, A.C., Coplen, T.B., 1998. The relative contribution of summer and cool-season precipitation to groundwater recharge, Spring Mountains, Nevada, USA. *Hydrogeology Journal* 6, 77–93.

Woodhouse, C.A., Meko, D.M., MacDonald, G.M., Stahle, D.W., Cook, E.R., 2010. A 1,200-year perspective of 21st century drought in southwestern North America. *Proceedings of the National Academy of Sciences of the United States of America* 107, 21283–21288. http://dx.doi.org/10.1073/pnas.0911197107.